

SUPPORTING INFORMATION

Design, synthesis and in-silico evaluation of newer 1,4-dihydropyridine based amlodipine bio-isosteres as promising antihypertensive agents

Priya Takkar^a, Bholey Singh^b, Balaram Pani^c, Rakesh Kumar^{a*}

^a *Bio-organic Laboratory, Department of Chemistry, University of Delhi, Delhi 110007, India*

^b *Swami Shraddhanand College, Alipur, University of Delhi, Delhi-110036*

^c *Bhaskaracharya College of Applied Sciences, Dwarka Sector-2, University of Delhi, New Delhi -110075*

* *Corresponding author*

Email: rakeshkp@email.com

CONTENTS

1. **Characterization Data of the synthesized compounds**
2. **¹H and ¹³C Spectra of the synthesized compounds**
3. **Single crystal X-ray Structures**
4. **Molecular Docking Assessment**
5. **In-silico ADMET Assessment**
6. **BOILED Egg Plot Analysis**

1. Characterization Data of the synthesized compounds:

3-Ethyl 5-methyl 4-(2-chlorophenyl)-6-methyl-2-((prop-2-yn-1-yloxy)methyl)-1,4-dihydropyridine-3,5-dicarboxylate (6). Yellow solid; Yield: 65%; mp: 111-113 °C ; IR (KBr, cm⁻¹); 3342, 2932, 1692, 1610, 1201; ¹H NMR (400 MHz, DMSO) δ 8.67 (s, 1H), 7.33 – 7.31 (m, 1H), 7.28 – 7.26 (m, 1H), 7.23 (dd, *J* = 7.5, 6.2 Hz, 1H), 7.12 (dd, *J* = 7.4, 6.0 Hz, 1H), 5.30 (s, 1H), 4.62 (d, *J* = 26.6 Hz, 2H), 4.22 (d, *J* = 2.4 Hz, 2H), 3.98 (dd, *J* = 7.1, 3.6 Hz, 2H), 3.53 (t, *J* = 2.4 Hz, 1H), 3.50 (s, 3H), 2.28 (s, 3H), 1.11 (s, 3H). ¹³C NMR (101 MHz, DMSO) δ 167.59, 166.76, 146.24, 146.11, 144.49, 131.50, 131.39, 129.45, 128.29, 127.94, 103.62, 101.98, 80.24, 78.31, 65.95, 59.93, 58.07, 50.98, 37.15, 18.58, 14.55; HRMS data: calcd mass (M+H)⁺ 404.1187, found, 404.1243.

3-Ethyl 5-methyl 4-(2-chlorophenyl)-2-(((1-(2-(2,3-dioxoindolin-1-yl)ethyl)-1H-1,2,3-triazol-4-yl)methoxy)methyl)-6-methyl-1,4-dihydropyridine-3,5-dicarboxylate (P1).

Orange solid; Yield: 92%; mp: 138-140 °C ; IR (KBr, cm^{-1}); 3342, 2932, 1751, 1685, 1610, 1220; ^1H NMR (400 MHz, DMSO) δ 8.57 (s, 1H), 8.23 (s, 1H), 7.57 (dd, $J = 7.8, 1.3$ Hz, 1H), 7.53 (d, $J = 6.8$ Hz, 1H), 7.32 (dd, $J = 7.8, 1.6$ Hz, 1H), 7.27 (dd, $J = 7.9, 1.2$ Hz, 1H), 7.22 (dd, $J = 7.5, 6.2$ Hz, 1H), 7.13 (dd, $J = 7.6, 1.6$ Hz, 1H), 7.09 – 7.05 (m, 1H), 6.93 (d, $J = 8.0$ Hz, 1H), 5.29 (s, 1H), 4.66 (d, $J = 6.0$ Hz, 2H), 4.54 (dd, $J = 7.7, 5.8$ Hz, 4H), 4.13 (d, $J = 5.7$ Hz, 2H), 3.98 – 3.94 (m, 2H), 3.34 (s, 3H), 2.27 (s, 3H), 1.09 (s, 3H). ^{13}C NMR (101 MHz, DMSO) δ 183.37, 167.60, 166.72, 158.59, 150.65, 146.28, 145.97, 145.01, 143.97, 138.55, 131.46, 129.44, 128.28, 127.92, 125.39, 124.99, 117.85, 110.73, 103.31, 102.07, 66.25, 63.76, 59.87, 50.99, 47.31, 37.16, 18.65, 14.53; HRMS data: calcd mass $(\text{M}+\text{H})^+$ 620.1834, found, 620.1922.

3-Ethyl 5-methyl 2-(((1-(2-(5-bromo-2,3-dioxoindolin-1-yl)ethyl)-1H-1,2,3-triazol-4-yl)methoxy)methyl)-4-(2-chlorophenyl)-6-methyl-1,4-dihydropyridine-3,5-dicarboxylate (P2)

Orange solid; Yield: 88%; mp: 136-138 °C ; IR (KBr, cm^{-1}); 3342, 2951, 1741, 1685, 1607, 1201; ^1H NMR (400 MHz, DMSO) δ 8.58 (s, 1H), 8.22 (s, 1H), 7.76 (dd, $J = 8.4, 2.1$ Hz, 1H), 7.70 (d, $J = 2.1$ Hz, 1H), 7.33 (dd, $J = 7.8, 1.7$ Hz, 1H), 7.26 (dd, $J = 7.9, 1.2$ Hz, 1H), 7.23 – 7.19 (m, 1H), 7.12 (dd, $J = 7.5, 5.9$ Hz, 1H), 6.90 (d, $J = 8.5$ Hz, 1H), 5.30 (s, 1H), 4.65 (s, 2H), 4.54 (dd, $J = 8.8, 4.6$ Hz, 4H), 4.13 (s, 2H), 3.96 (dd, $J = 7.1, 3.5$ Hz, 2H), 3.50 (s, 3H), 2.27 (s, 3H), 1.10 (s, 3H). ^{13}C NMR (101 MHz, DMSO) δ 182.15, 167.62, 166.74, 158.21, 149.55, 146.27, 145.95, 145.01, 144.01, 140.25, 131.48, 129.43, 128.28, 127.92, 127.25, 125.42, 119.58, 115.56, 112.90, 103.34, 102.10, 66.24, 63.75, 59.89, 50.99, 47.27, 37.17, 18.66, 14.53; HRMS data: calcd mass $(\text{M}+\text{H})^+$ 698.0939, found, 698.0998.

3-Ethyl 5-methyl 2-(((1-(2-(5-chloro-2,3-dioxoindolin-1-yl)ethyl)-1H-1,2,3-triazol-4-yl)methoxy)methyl)-4-(2-chlorophenyl)-6-methyl-1,4-dihydropyridine-3,5-dicarboxylate (P3)

Orange solid; Yield: 90%; mp: 138-140 °C ; IR (KBr, cm^{-1}); 3342, 2932, 1739, 1692, 1610, 1201; ^1H NMR (400 MHz, DMSO) δ 8.58 (s, 1H), 8.22 (s, 1H), 7.64 – 7.62 (m, 1H), 7.60 (d, $J = 2.1$ Hz, 1H), 7.32 (d, $J = 6.2$ Hz, 1H), 7.26 (d, $J = 6.9$ Hz, 1H), 7.20 (d, $J = 7.5$ Hz, 1H), 7.13 – 7.10 (m, 1H), 6.94 (s, 1H), 5.29 (s, 1H), 4.65 (s, 2H), 4.55 – 4.52 (m, 4H), 4.14 (s, 2H), 3.97 – 3.94 (m, 2H), 3.50 (s, 3H), 2.27 (s, 3H), 1.09 (s, 3H). ^{13}C NMR (101 MHz, DMSO) δ 182.29, 167.60, 166.73, 158.38, 149.19, 146.29, 145.96, 145.01, 144.00, 137.42, 131.48, 129.43, 128.26, 128.03, 128.33, 127.81, 125.43, 124.51, 119.23, 112.48, 103.35, 102.09, 66.25,

63.77, 59.87, 50.98, 47.28, 37.17, 18.66, 14.53; HRMS data: calcd mass (M+H)⁺ 654.1444, found, 654.1539.

3-Ethyl 5-methyl 4-(2-chlorophenyl)-2-(((1-(2-(5-fluoro-2,3-dioxindolin-1-yl)ethyl)-1H-1,2,3-triazol-4-yl)methoxy)methyl)-6-methyl-1,4-dihydropyridine-3,5-dicarboxylate (P4)

Orange solid; Yield: 90%; mp: 140-142 °C ; IR (KBr, cm⁻¹); 3355, 2947, 1759, 1698, 1602, 1207; ¹H NMR (400 MHz, DMSO) δ 8.57 (s, 1H), 8.22 (s, 1H), 7.49 – 7.46 (m, 1H), 7.46 – 7.44 (m, 1H), 7.33 – 7.31 (m, 1H), 7.28 – 7.25 (m, 1H), 7.21 (dd, *J* = 7.5, 6.2 Hz, 1H), 7.12 (dd, *J* = 7.5, 5.9 Hz, 1H), 6.97 – 6.94 (m, 1H), 5.29 (s, 1H), 4.65 (s, 2H), 4.54 (dd, *J* = 7.2, 3.7 Hz, 4H), 4.13 (d, *J* = 5.7 Hz, 2H), 3.96 (dd, *J* = 7.1, 3.4 Hz, 2H), 3.50 (s, 3H), 2.27 (s, 3H), 1.09 (s, 3H). ¹³C NMR (101 MHz, DMSO) δ 182.79, 167.63, 166.74, 158.62, 157.73, 146.88, 146.25, 145.95, 145.00, 144.00, 131.46, 129.43, 128.29, 127.91, 125.41, 124.64, 124.40, 118.72, 112.24, 112.10, 103.29, 102.08, 66.23, 63.73, 59.89, 50.99, 47.27, 37.16, 18.63, 14.51; HRMS data: calcd mass (M+H)⁺ 638.1740, found, 638.1859.

3-Ethyl 5-methyl 4-(2-chlorophenyl)-2-(((1-(2-(3-formyl-1H-indol-1-yl)ethyl)-1H-1,2,3-triazol-4-yl)methoxy)methyl)-6-methyl-1,4-dihydropyridine-3,5-dicarboxylate (P5)

Orange solid; Yield: 92%; mp: 145-147 °C ; IR (KBr, cm⁻¹); 3379, 2947, 1746, 1692, 1610, 1218; ¹H NMR (400 MHz, DMSO) δ 9.82 (s, 1H), 8.59 (s, 1H), 8.07 (dd, *J* = 7.0, 1.2 Hz, 1H), 8.03 (s, 1H), 8.02 (s, 1H), 7.52 (d, *J* = 7.7 Hz, 1H), 7.32 (dd, *J* = 7.8, 1.6 Hz, 1H), 7.27 (dd, *J* = 7.7, 1.2 Hz, 2H), 7.24 – 7.23 (m, 1H), 7.21 – 7.19 (m, 1H), 7.14 – 7.10 (m, 1H), 5.30 (s, 1H), 4.87 (d, *J* = 5.8 Hz, 2H), 4.82 (d, *J* = 5.8 Hz, 2H), 4.54 (dd, *J* = 7.9, 5.8 Hz, 4H), 3.98 – 3.93 (m, 2H), 3.50 (s, 3H), 2.27 (s, 3H), 1.09 (s, 3H). ¹³C NMR (101 MHz, DMSO) δ 185.16, 167.64, 166.75, 146.24, 145.96, 145.04, 144.01, 141.08, 137.36, 131.46, 129.45, 128.30, 127.90, 124.95, 124.11, 123.05, 121.47, 118.02, 111.09, 103.24, 102.08, 66.20, 63.68, 59.90, 51.00, 49.49, 46.72, 37.16, 18.63, 14.50; HRMS data: calcd mass (M+H)⁺ 618.2041, found, 618.2167.

3-Ethyl 5-methyl 4-(2-chlorophenyl)-6-methyl-2-(((1-phenyl-1H-1,2,3-triazol-4-yl)methoxy)methyl)-1,4-dihydropyridine-3,5-dicarboxylate (P6). White solid; Yield: 95%;

mp: 125-127 °C ; IR (KBr, cm⁻¹); 3373, 2897, 1695, 1605, 1276; ¹H NMR (400 MHz, DMSO) δ 8.85 (s, 1H), 8.68 (s, 1H), 7.90 (d, *J* = 7.5 Hz, 2H), 7.63 – 7.60 (m, 2H), 7.52 – 7.49 (m, 1H), 7.35 – 7.32 (m, 1H), 7.27 (dd, *J* = 7.9, 1.2 Hz, 1H), 7.21 (dd, *J* = 7.5, 6.3 Hz, 1H), 7.12 (dd, *J* = 7.5, 5.9 Hz, 1H), 5.31 (s, 1H), 4.76 – 4.71 (m, 3H), 4.62 (d, *J* = 13.6 Hz, 1H), 3.99 – 3.94 (m, 2H), 3.49 (s, 3H), 2.29 (s, 3H), 1.09 (s, 3H). ¹³C NMR (101 MHz, DMSO) δ 167.59, 166.78, 146.26, 146.03, 144.98, 137.08, 131.47, 130.39, 129.44, 129.17, 128.27, 127.92, 122.92,

120.53, 103.59, 102.01, 66.47, 63.85, 59.90, 50.96, 37.21, 18.65, 14.50; HRMS data: calcd mass (M+H)⁺ 523.1670, found, 523.1748.

3-Ethyl 5-methyl 4-(2-chlorophenyl)-2-(((1-(4-fluorophenyl)-1H-1,2,3-triazol-4-yl)methoxy)methyl)-6-methyl-1,4-dihydropyridine-3,5-dicarboxylate (P7). White solid; Yield: 96%; mp: 125-127 °C ; IR (KBr, cm⁻¹); 3342, 2932, 1692, 1610, 1201; ¹H NMR (400 MHz, DMSO) δ 8.83 (s, 1H), 8.69 (s, 1H), 7.97 – 7.95 (m, 1H), 7.95 – 7.93 (m, 1H), 7.47 (dd, *J* = 11.0, 4.3 Hz, 2H), 7.33 (dd, *J* = 7.8, 1.6 Hz, 1H), 7.28 – 7.26 (m, 1H), 7.22 (dd, *J* = 7.5, 6.3 Hz, 1H), 7.12 (dd, *J* = 7.5, 6.0 Hz, 1H), 5.30 (s, 1H), 4.72 (dd, *J* = 9.9, 5.4 Hz, 3H), 4.61 (d, *J* = 13.6 Hz, 1H), 3.96 (dd, *J* = 7.1, 2.4 Hz, 2H), 3.49 (s, 3H), 2.29 (s, 3H), 1.09 (s, 3H). ¹³C NMR (101 MHz, DMSO) δ 167.58, 166.77, 146.25, 146.04, 145.11, 144.86, 133.63, 131.47, 129.44, 128.27, 127.91, 123.16, 122.87, 117.34, 117.11, 103.61, 102.00, 66.47, 63.82, 59.90, 50.96, 37.20, 18.65, 14.49; HRMS data: calcd mass (M+H)⁺ 541.1576, found, 541.1651.

3-Ethyl 5-methyl 4-(2-chlorophenyl)-2-(((1-(4-chlorophenyl)-1H-1,2,3-triazol-4-yl)methoxy)methyl)-6-methyl-1,4-dihydropyridine-3,5-dicarboxylate (P8). White solid; Yield: 96%; mp: 123-125 °C ; IR (KBr, cm⁻¹); 3373, 2920, 1695, 1607, 1287; ¹H NMR (400 MHz, DMSO) δ 8.88 (s, 1H), 8.69 (s, 1H), 7.96 – 7.94 (m, 2H), 7.70 – 7.68 (m, 2H), 7.33 (dd, *J* = 7.8, 1.7 Hz, 1H), 7.26 (dd, *J* = 7.9, 1.2 Hz, 1H), 7.21 (dt, *J* = 7.6, 3.7 Hz, 1H), 7.14 – 7.09 (m, 1H), 5.29 (s, 1H), 4.75 – 4.70 (m, 3H), 4.61 (d, *J* = 13.5 Hz, 1H), 3.98 – 3.94 (m, 2H), 3.49 (s, 3H), 2.28 (s, 3H), 1.09 (s, 3H). ¹³C NMR (101 MHz, DMSO) δ 167.57, 166.77, 146.25, 146.05, 145.25, 144.84, 135.87, 133.42, 131.46, 130.37, 129.44, 128.28, 127.92, 123.02, 122.19, 103.64, 101.98, 66.47, 63.79, 59.90, 50.96, 37.19, 31.43, 22.54, 18.65, 14.50; HRMS data: calcd mass (M+H)⁺ 557.1280, found, 557.1357.

3-Ethyl 5-methyl 2-(((1-(4-bromophenyl)-1H-1,2,3-triazol-4-yl)methoxy)methyl)-4-(2-chlorophenyl)-6-methyl-1,4-dihydropyridine-3,5-dicarboxylate (P9). White solid; Yield: 94%; mp: 124-126 °C ; IR (KBr, cm⁻¹); 3361, 2874, 1684, 1602, 1280; ¹H NMR (400 MHz, DMSO) δ 8.87 (s, 1H), 8.66 (s, 1H), 7.89 (d, *J* = 9.0 Hz, 2H), 7.82 (d, *J* = 9.0 Hz, 2H), 7.34 – 7.32 (m, 1H), 7.28 – 7.25 (m, 1H), 7.21 (dd, *J* = 7.5, 6.2 Hz, 1H), 7.12 (dd, *J* = 7.5, 5.9 Hz, 1H), 5.30 (s, 1H), 4.74 (dd, *J* = 13.1, 4.2 Hz, 3H), 4.61 (d, *J* = 13.6 Hz, 1H), 3.99 – 3.94 (m, 2H), 3.49 (s, 3H), 2.29 (s, 3H), 1.09 (d, *J* = 2.6 Hz, 3H). ¹³C NMR (101 MHz, DMSO) δ 167.57, 166.77, 146.23, 146.01, 145.27, 144.83, 136.28, 133.29, 131.47, 129.44, 128.27, 127.90, 122.96, 122.43, 121.80, 103.62, 102.00, 66.49, 65.38, 63.81, 59.90, 50.95, 37.22, 31.42, 22.53, 18.65, 15.63, 14.49; HRMS data: calcd mass (M+H)⁺ 601.0775, found, 601.0852.

3-Ethyl 5-methyl 4-(2-chlorophenyl)-2-(((1-(4-iodophenyl)-1H-1,2,3-triazol-4-yl)methoxy)methyl)-6-methyl-1,4-dihydropyridine-3,5-dicarboxylate (P10). White solid; Yield: 94%; mp: 125-127 °C ; IR (KBr, cm⁻¹); 3361, 2899, 1692, 1610, 1201; ¹H NMR (400 MHz, DMSO) δ 8.86 (s, 1H), 8.67 (s, 1H), 7.97 (d, *J* = 8.8 Hz, 2H), 7.72 (s, 2H), 7.34 – 7.31 (m, 1H), 7.28 – 7.25 (m, 1H), 7.21 (dd, *J* = 7.5, 6.2 Hz, 1H), 7.12 (dd, *J* = 7.5, 5.9 Hz, 1H), 5.29 (s, 1H), 4.75 – 4.70 (m, 3H), 4.60 (d, *J* = 13.6 Hz, 1H), 3.96 (dd, *J* = 7.1, 2.4 Hz, 2H), 3.49 (s, 3H), 2.28 (s, 3H), 1.08 (s, 3H). ¹³C NMR (101 MHz,) δ 167.63, 166.83, 146.30, 146.08, 145.32, 144.89, 139.15, 136.79, 131.53, 129.50, 128.15, 127.93, 127.82, 122.90, 122.45, 103.68, 102.05, 94.85, 66.54, 63.87, 59.96, 51.02, 31.48, 22.59, 18.71, 15.69, 14.55; HRMS data: calcd mass (M+H)⁺ 649.0636, found, 649.0686.

3-Ethyl 5-methyl 4-(2-chlorophenyl)-6-methyl-2-(((1-(4-nitrophenyl)-1H-1,2,3-triazol-4-yl)methoxy)methyl)-1,4-dihydropyridine-3,5-dicarboxylate (P11). White solid; Yield: 93%; mp: 127-128 °C ; IR (KBr, cm⁻¹); 3342, 2932, 1692, 1610, 1287; ¹H NMR (400 MHz, DMSO) δ 9.07 (s, 1H), 8.69 (s, 1H), 8.47 (d, *J* = 9.2 Hz, 2H), 8.24 (d, *J* = 9.2 Hz, 2H), 7.34 – 7.32 (m, 1H), 7.28 – 7.25 (m, 1H), 7.22 (dd, *J* = 7.5, 6.3 Hz, 1H), 7.12 (dd, *J* = 7.5, 6.0 Hz, 1H), 5.29 (s, 1H), 4.74 (d, *J* = 2.7 Hz, 3H), 4.62 (d, *J* = 13.5 Hz, 1H), 3.97 (dd, *J* = 7.1, 2.4 Hz, 2H), 3.49 (s, 3H), 2.29 (s, 3H), 1.09 (s, 3H). ¹³C NMR (101 MHz, DMSO) δ 167.57, 166.77, 146.23, 146.01, 145.27, 144.83, 136.28, 133.29, 131.47, 129.44, 128.27, 127.90, 122.96, 122.43, 121.80, 103.62, 102.00, 66.49, 65.38, 63.81, 59.90, 50.95, 37.22, 31.42, 22.53, 18.65, 15.63, 14.49; HRMS data: calcd mass (M+H)⁺ 568.1521, found, 568.1590.

3-Ethyl 5-methyl 4-(2-chlorophenyl)-2-(((1-(2-fluorophenyl)-1H-1,2,3-triazol-4-yl)methoxy)methyl)-6-methyl-1,4-dihydropyridine-3,5-dicarboxylate (P12). White solid; Yield: 92%; mp: 126-128 °C ; IR (KBr, cm⁻¹); 3349, 2920, 1684, 1605, 1265; ¹H NMR (400 MHz, DMSO) δ 8.70 (s, 1H), 8.64 (d, *J* = 2.1 Hz, 1H), 7.84 (dd, *J* = 7.8, 6.3 Hz, 1H), 7.62 – 7.56 (m, 2H), 7.48 – 7.44 (m, 1H), 7.34 – 7.32 (m, 1H), 7.28 – 7.25 (m, 1H), 7.21 (dt, *J* = 7.7, 3.7 Hz, 1H), 7.12 (dd, *J* = 7.4, 6.0 Hz, 1H), 5.31 (s, 1H), 4.73 (d, *J* = 2.3 Hz, 3H), 4.63 (d, *J* = 13.6 Hz, 1H), 3.97 (dd, *J* = 7.1, 2.7 Hz, 2H), 3.50 (s, 3H), 2.29 (s, 3H), 1.10 (s, 3H). ¹³C NMR (101 MHz, DMSO) δ 167.59, 166.79, 155.49, 153.00, 146.26, 146.05, 144.87, 144.64, 131.61, 129.44, 128.27, 127.91, 126.53, 125.94, 125.20, 117.64, 103.60, 102.00, 66.51, 63.69, 59.90, 50.96, 37.21, 18.63, 14.50; HRMS data: calcd mass (M+H)⁺ 541.1576, found, 541.1650.

3-Ethyl 5-methyl 4-(2-chlorophenyl)-2-(((1-(2-methoxy-4-nitrophenyl)-1H-1,2,3-triazol-4-yl)methoxy)methyl)-6-methyl-1,4-dihydropyridine-3,5-dicarboxylate (P13). White solid; Yield: 91%; mp: 130-132 °C ; IR (KBr, cm⁻¹); 3361, 2932, 1696, 1610, 1271; ¹H NMR (400 MHz, DMSO) δ 8.70 (s, 1H), 8.68 (s, 1H), 8.09 (s, 1H), 8.04 (s, 2H), 7.34 – 7.32 (m, 1H), 7.28 – 7.26 (m, 1H), 7.21 (t, *J* = 7.0 Hz, 1H), 7.12 (dd, *J* = 7.4, 6.1 Hz, 1H), 5.30 (s, 1H), 4.73 (d, *J* = 2.6 Hz, 3H), 4.63 (d, *J* = 13.7 Hz, 1H), 4.03 (s, 3H), 3.98 (dd, *J* = 7.1, 2.6 Hz, 2H), 3.49 (s, 3H), 2.29 (s, 3H), 1.10 (s, 3H). ¹³C NMR (101 MHz, DMSO) δ 167.58, 166.81, 151.81, 148.58, 146.15, 144.88, 144.38, 131.47, 130.95, 129.44, 128.28, 127.91, 126.59, 126.24, 116.78, 108.87, 103.62, 101.97, 66.46, 63.66, 59.91, 57.59, 50.96, 37.20, 18.63, 14.51; HRMS data: calcd mass (M+H)⁺ 598.1626, found, 598.1693.

3-Ethyl 5-methyl 4-(2-chlorophenyl)-2-(((1-(3-cyanophenyl)-1H-1,2,3-triazol-4-yl)methoxy)methyl)-6-methyl-1,4-dihydropyridine-3,5-dicarboxylate (P14). White solid; Yield: 96%; mp: 128-130 °C ; IR (KBr, cm⁻¹); 3373, 2932, 1695, 1605, 1287; ¹H NMR (400 MHz, DMSO) δ 8.94 (s, 1H), 8.66 (s, 1H), 8.44 – 8.43 (m, 1H), 8.30 (ddd, *J* = 8.3, 2.3, 1.0 Hz, 1H), 8.00 – 7.97 (m, 1H), 7.83 (t, *J* = 8.0 Hz, 1H), 7.33 (dd, *J* = 7.8, 1.7 Hz, 1H), 7.27 (dd, *J* = 7.9, 1.3 Hz, 1H), 7.22 (td, *J* = 7.5, 1.3 Hz, 1H), 7.14 – 7.10 (m, 1H), 5.30 (s, 1H), 4.75 (t, *J* = 9.5 Hz, 3H), 4.61 (d, *J* = 13.5 Hz, 1H), 3.97 (dd, *J* = 7.1, 2.3 Hz, 2H), 3.49 (s, 3H), 2.29 (s, 3H), 1.10 (d, *J* = 7.1 Hz, 3H). ¹³C NMR (101 MHz, DMSO) δ 167.57, 166.77, 146.22, 146.00, 145.44, 144.80, 137.49, 132.75, 131.81, 131.48, 129.45, 128.26, 127.90, 125.15, 123.88, 123.17, 118.27, 113.30, 103.67, 101.99, 66.52, 63.80, 59.90, 50.94, 37.25, 18.65, 14.49; HRMS data: calcd mass (M+H)⁺ 548.1622, found, 548.1678.

2. ^1H and ^{13}C NMR Spectra of the synthesized compounds:

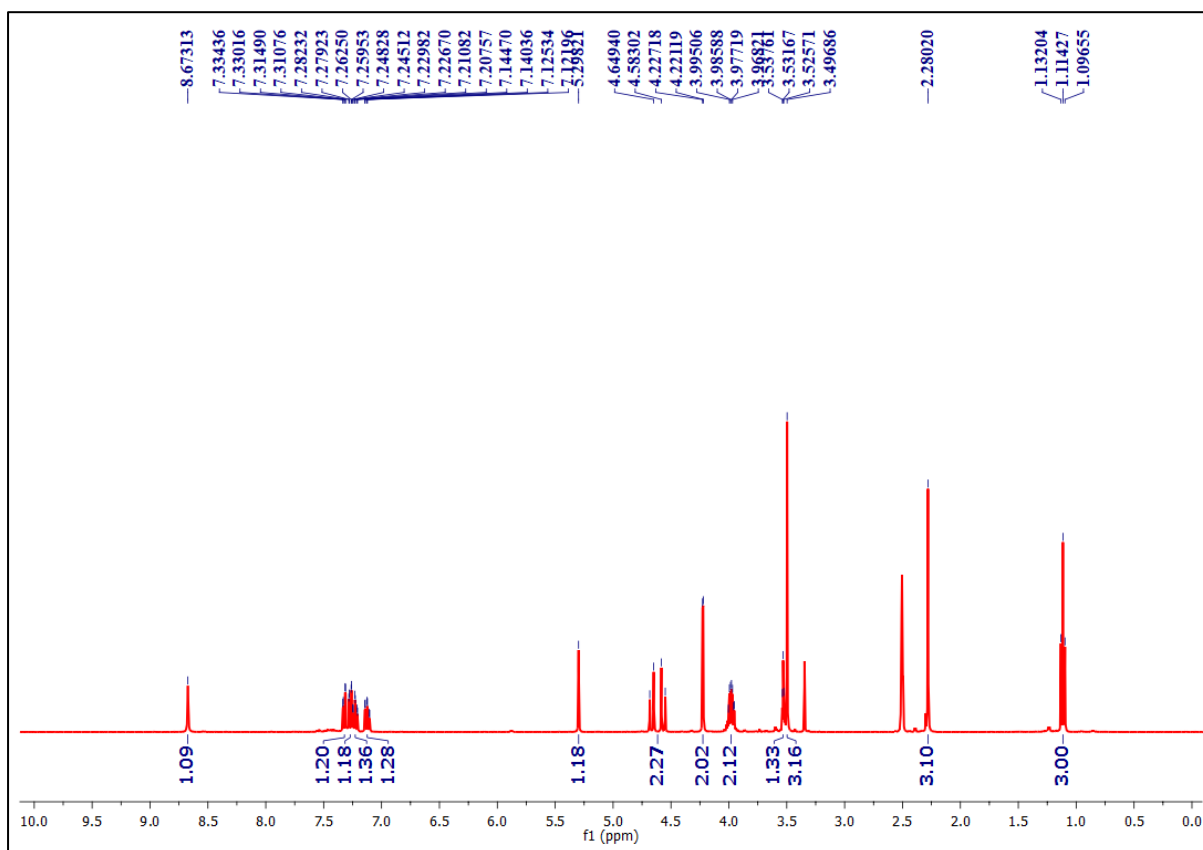


Figure S1. ^1H NMR spectrum of compound 6 (400 MHz, $\text{DMSO-}d_6$).

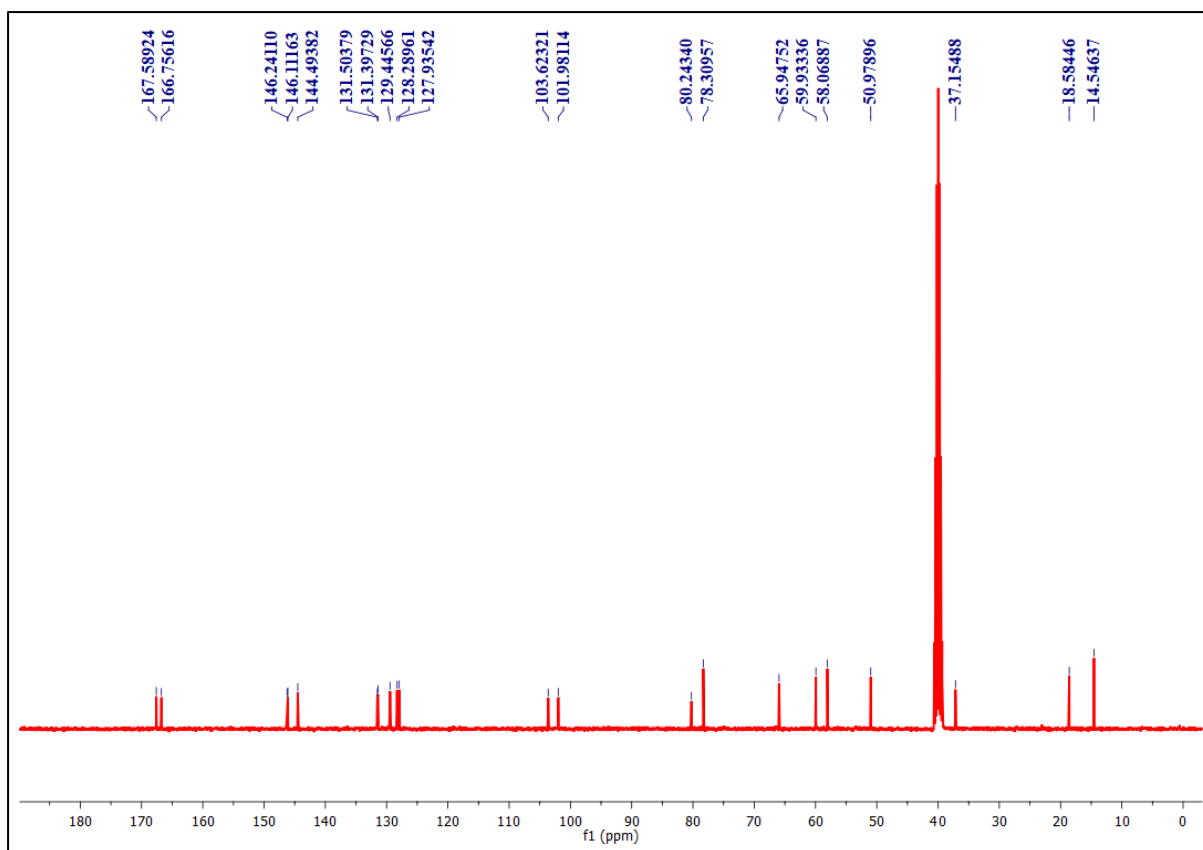


Figure S2. ^{13}C NMR spectrum of compound **6** (100 MHz, $\text{DMSO-}d_6$).

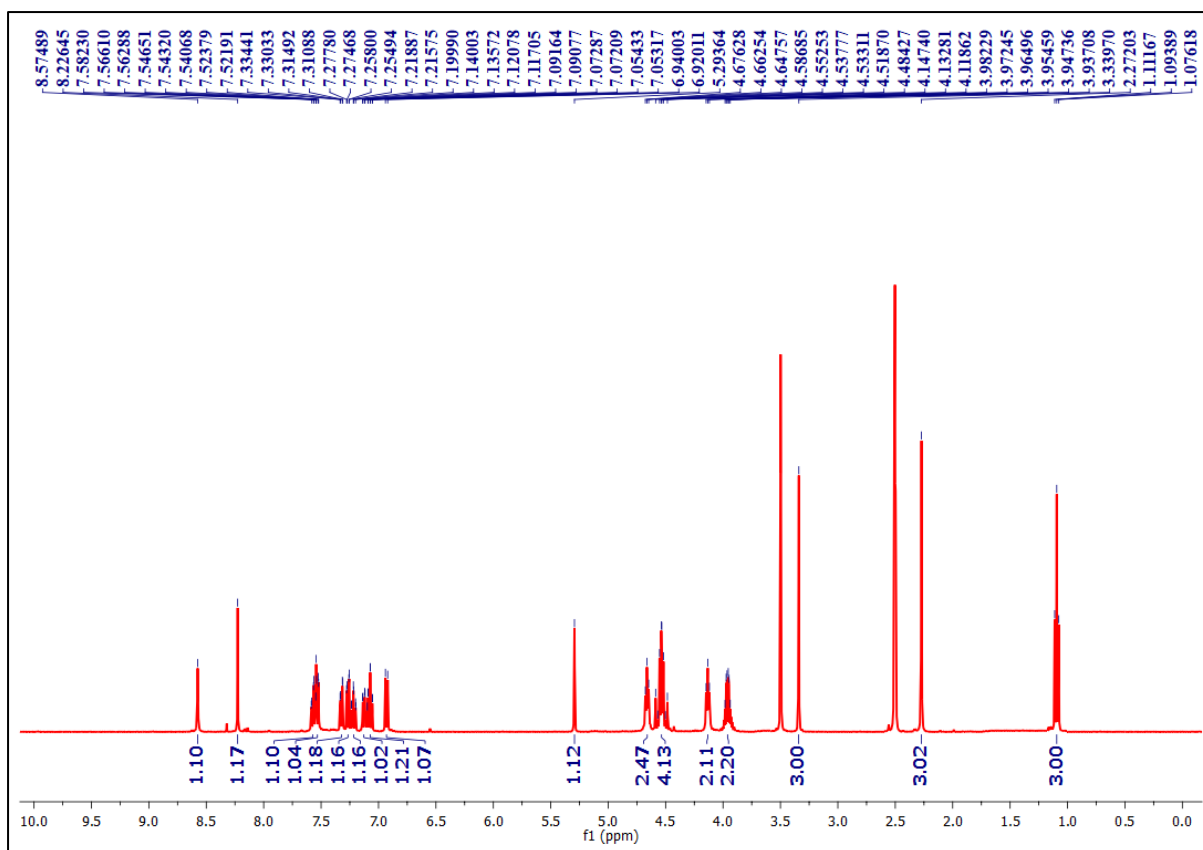


Figure S3. ^1H NMR spectrum of compound P1 (400 MHz, DMSO- d_6).

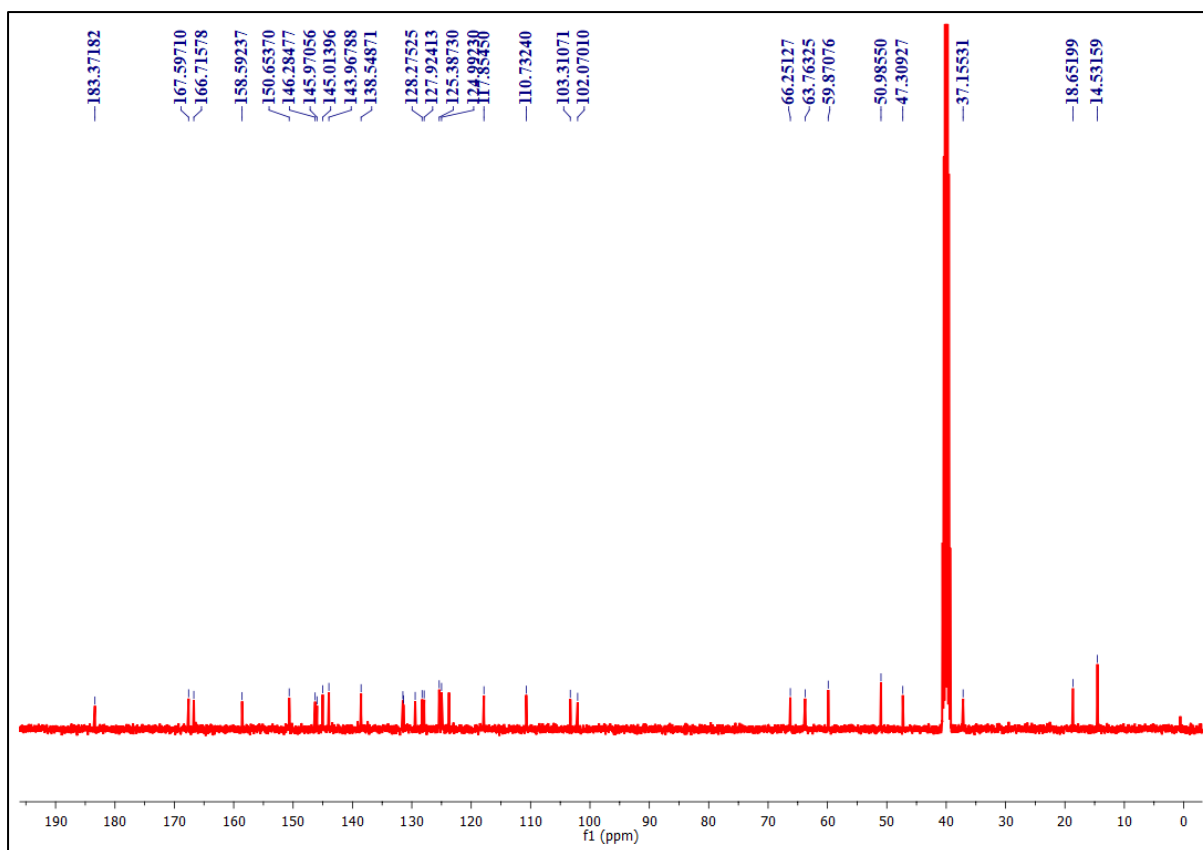


Figure S4. ^{13}C NMR spectrum of compound P1 (100 MHz, DMSO- d_6).

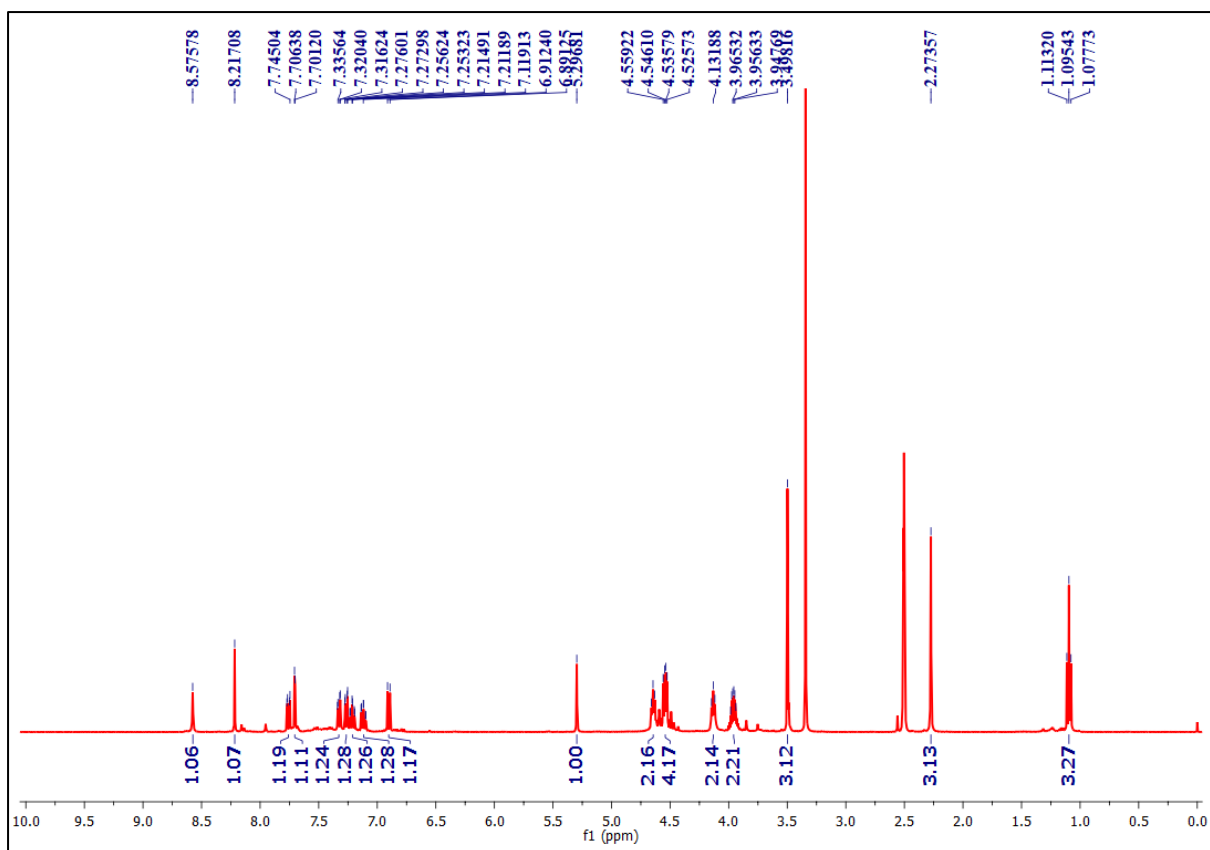


Figure S5. ^1H NMR spectrum of compound **P2** (400 MHz, $\text{DMSO-}d_6$).

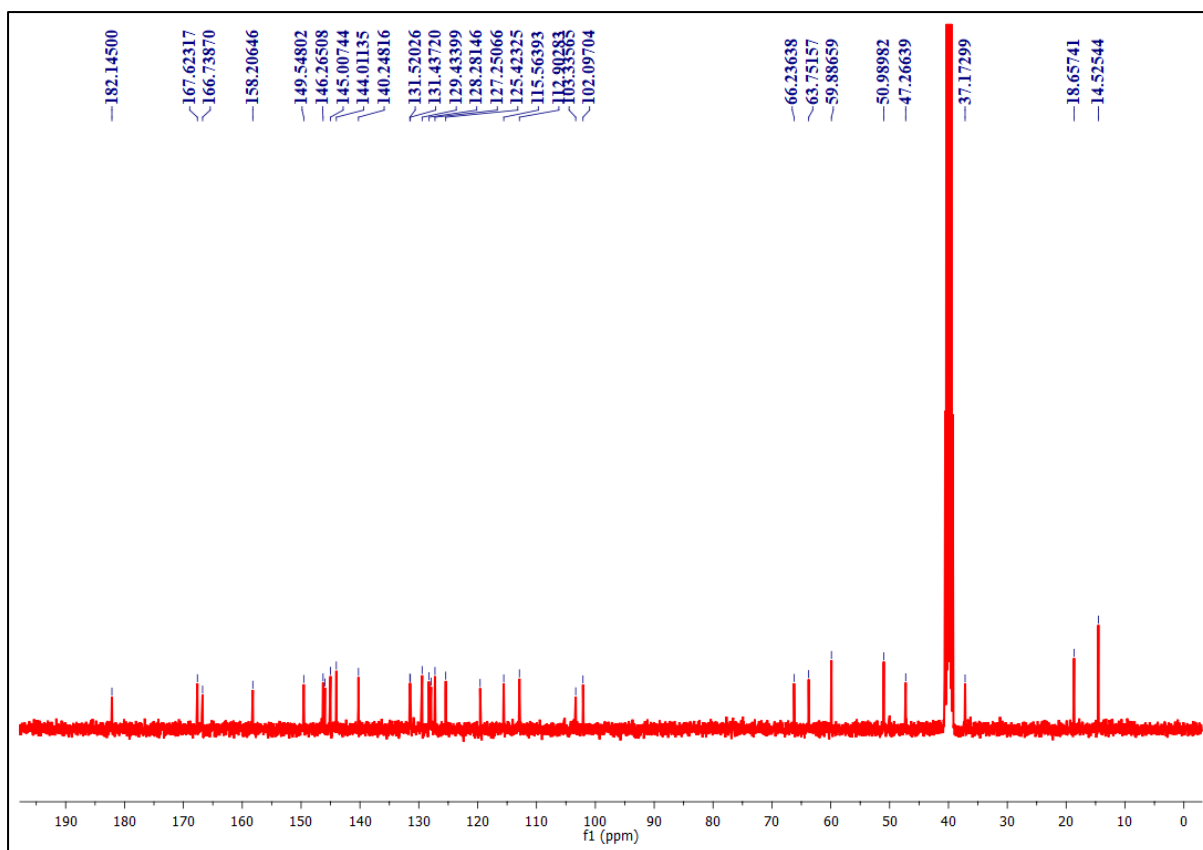


Figure S6. ^{13}C NMR spectrum of compound P2 (100 MHz, DMSO-*d*₆).

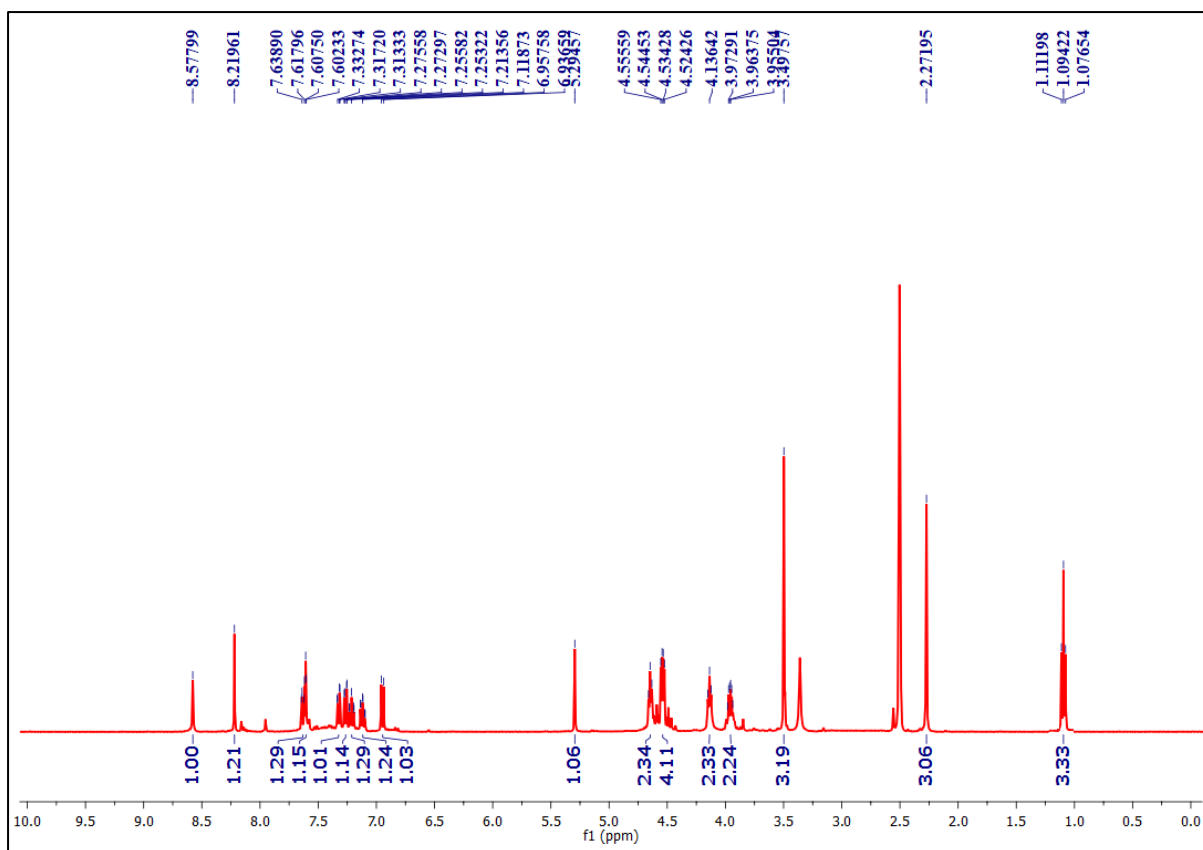


Figure S7. ^1H NMR spectrum of compound **P3** (400 MHz, $\text{DMSO-}d_6$).

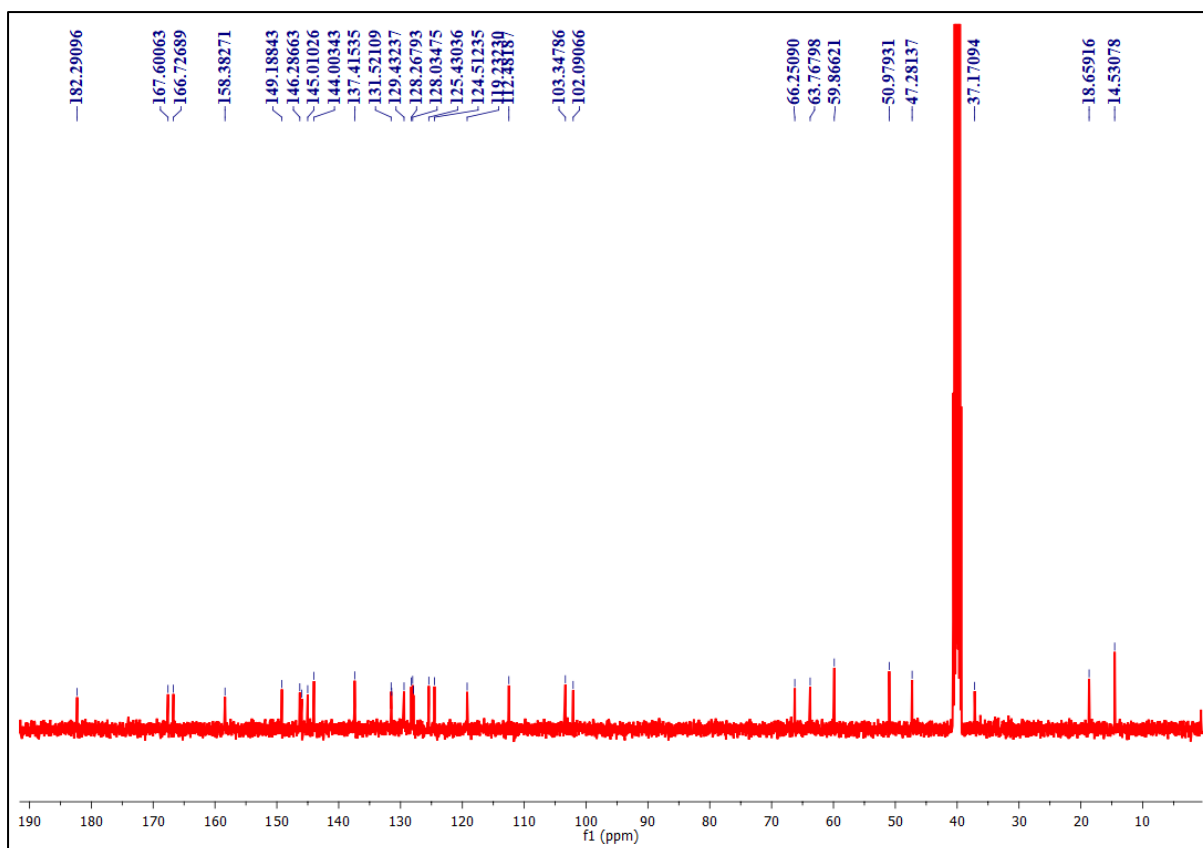


Figure S8. ^{13}C NMR spectrum of compound **P3** (100 MHz, $\text{DMSO-}d_6$).

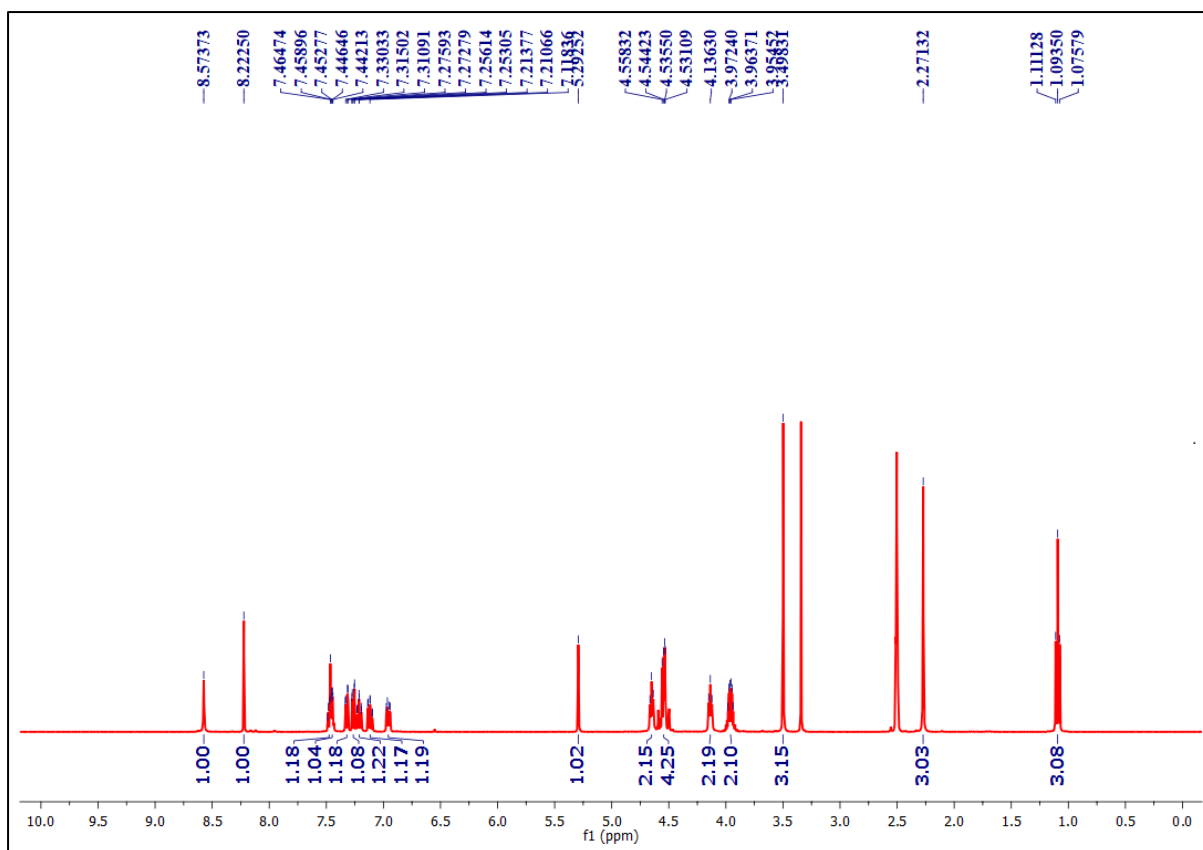


Figure S9. ¹H NMR spectrum of compound **P4** (400 MHz, DMSO-*d*₆).

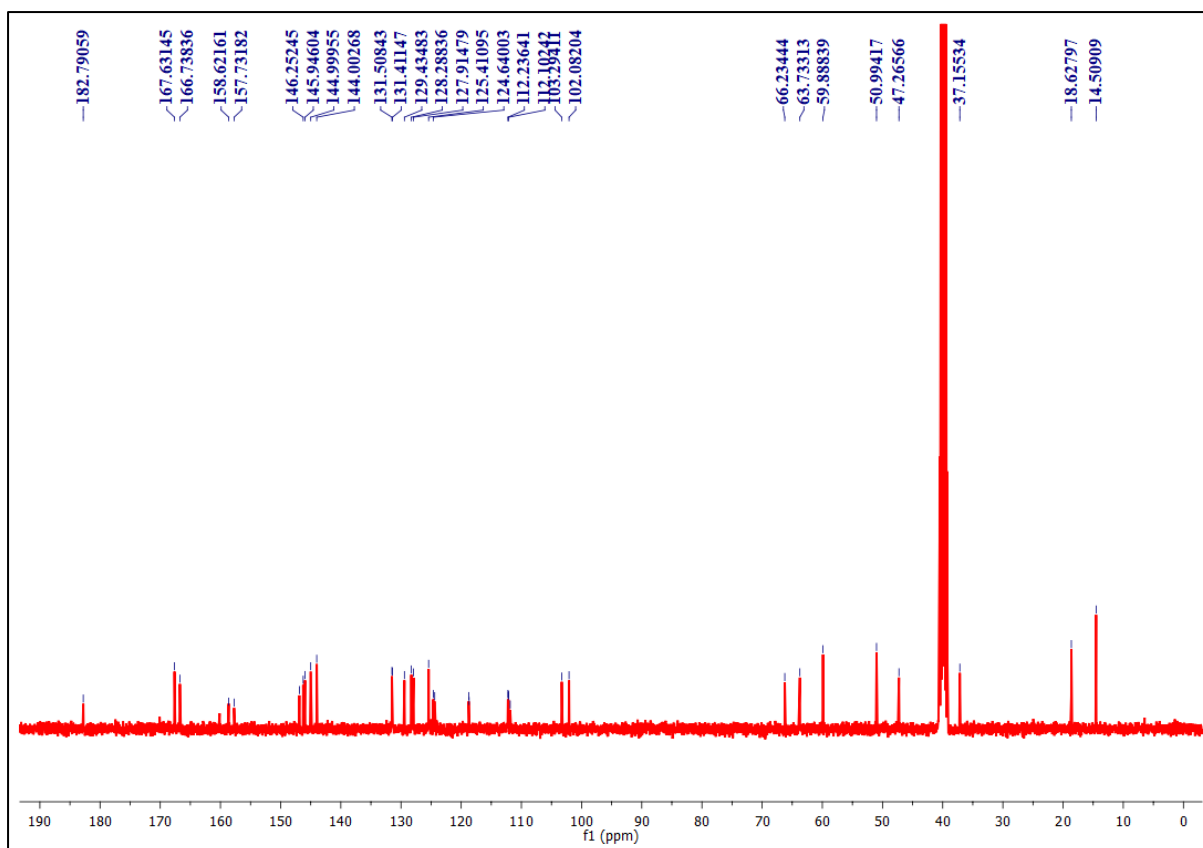


Figure S10. ^{13}C NMR spectrum of compound **P4** (100 MHz, DMSO- d_6).

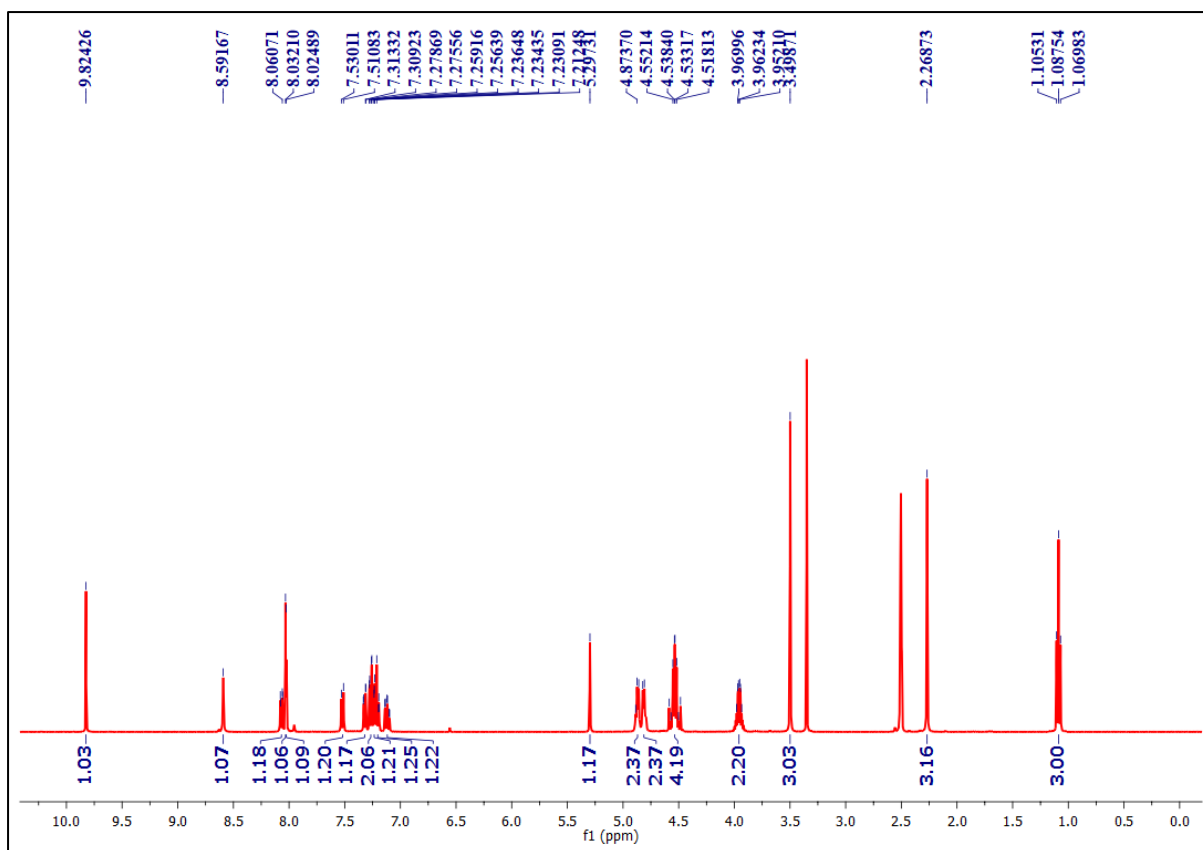


Figure S11. ^1H NMR spectrum of compound **P5** (400 MHz, $\text{DMSO-}d_6$).

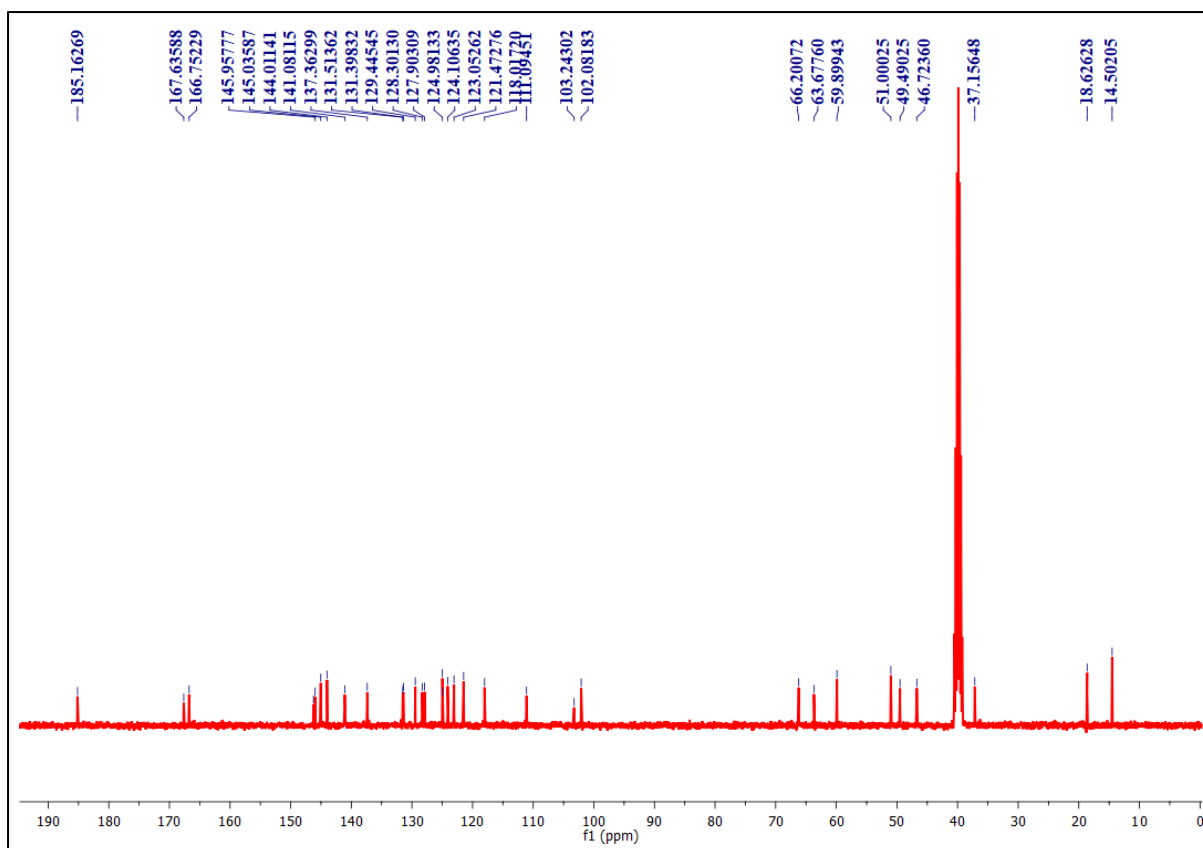


Figure S12. ^{13}C NMR spectrum of compound **P5** (100 MHz, $\text{DMSO-}d_6$).

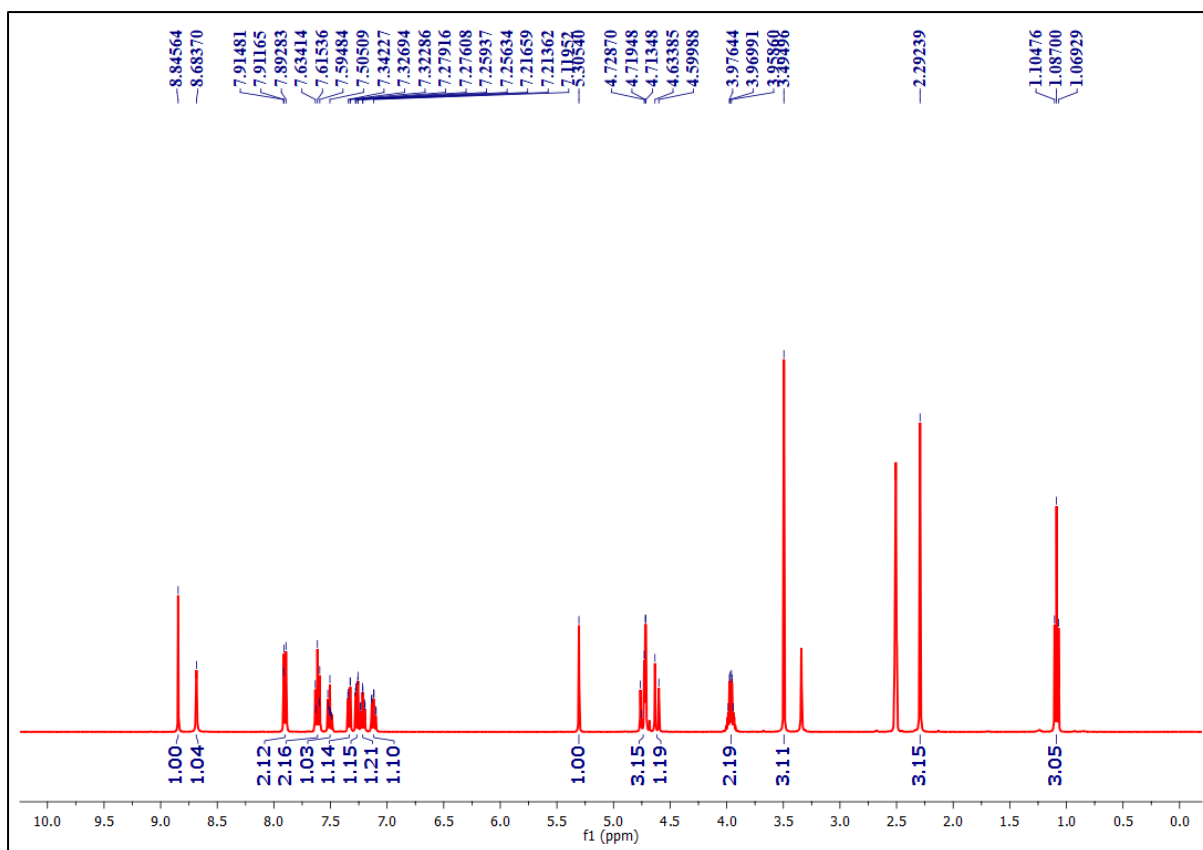


Figure S13. ¹H NMR spectrum of compound P6 (400 MHz, DMSO-*d*₆).

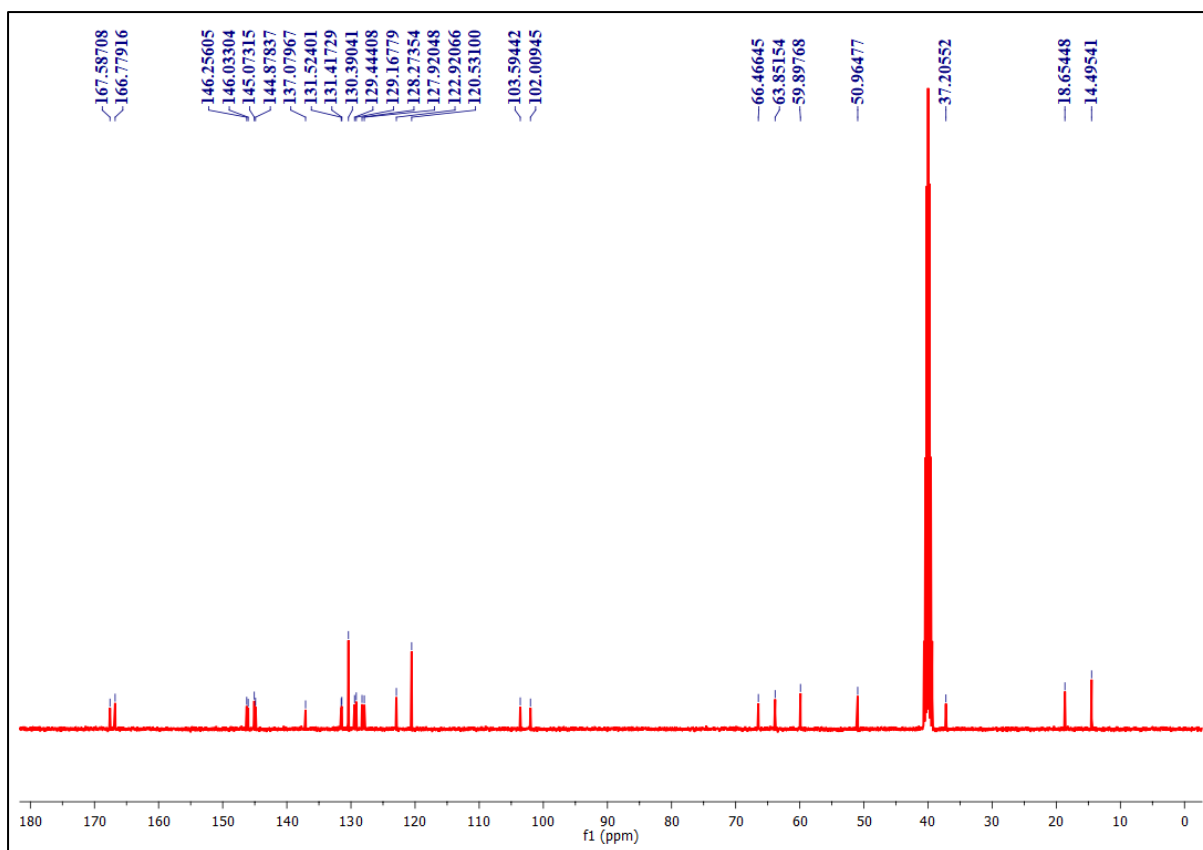


Figure S14. ^{13}C NMR spectrum of compound P6 (100 MHz, $\text{DMSO-}d_6$).

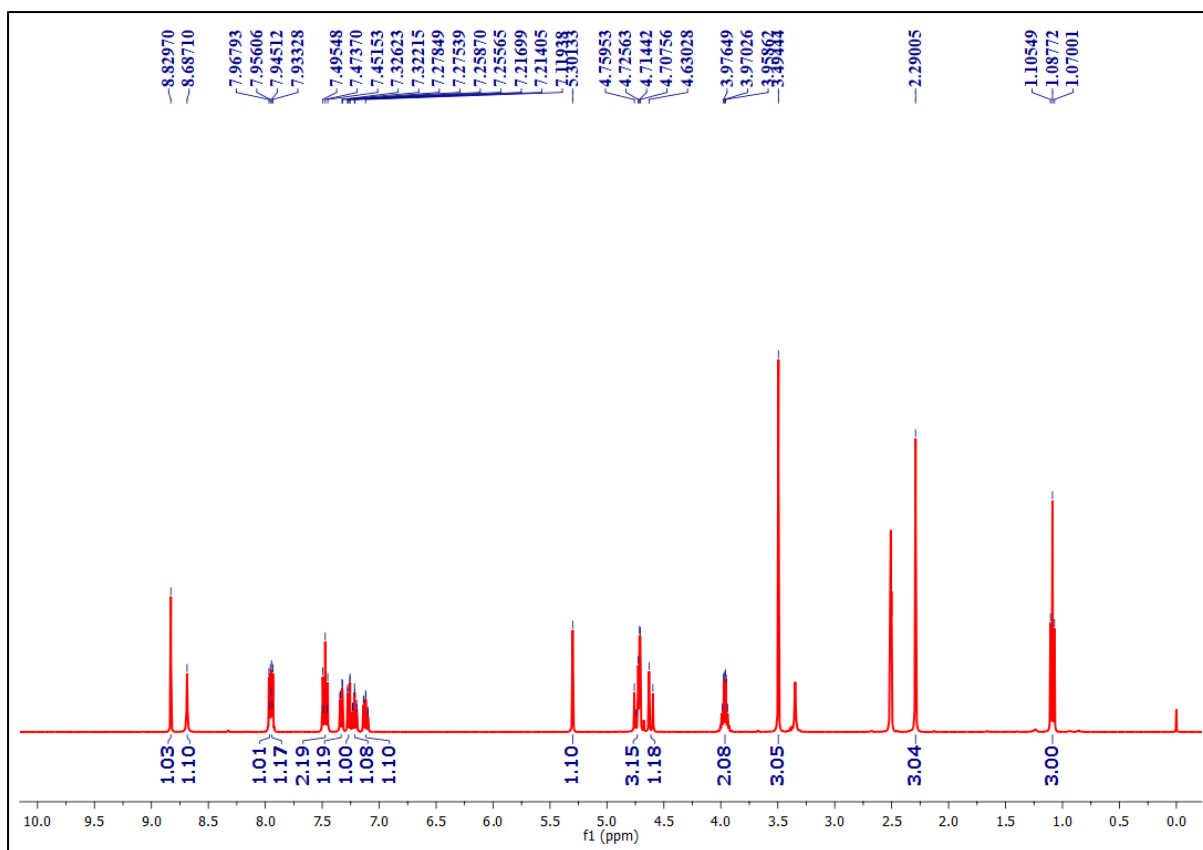


Figure S15. ¹H NMR spectrum of compound P7 (400 MHz, DMSO-*d*₆).

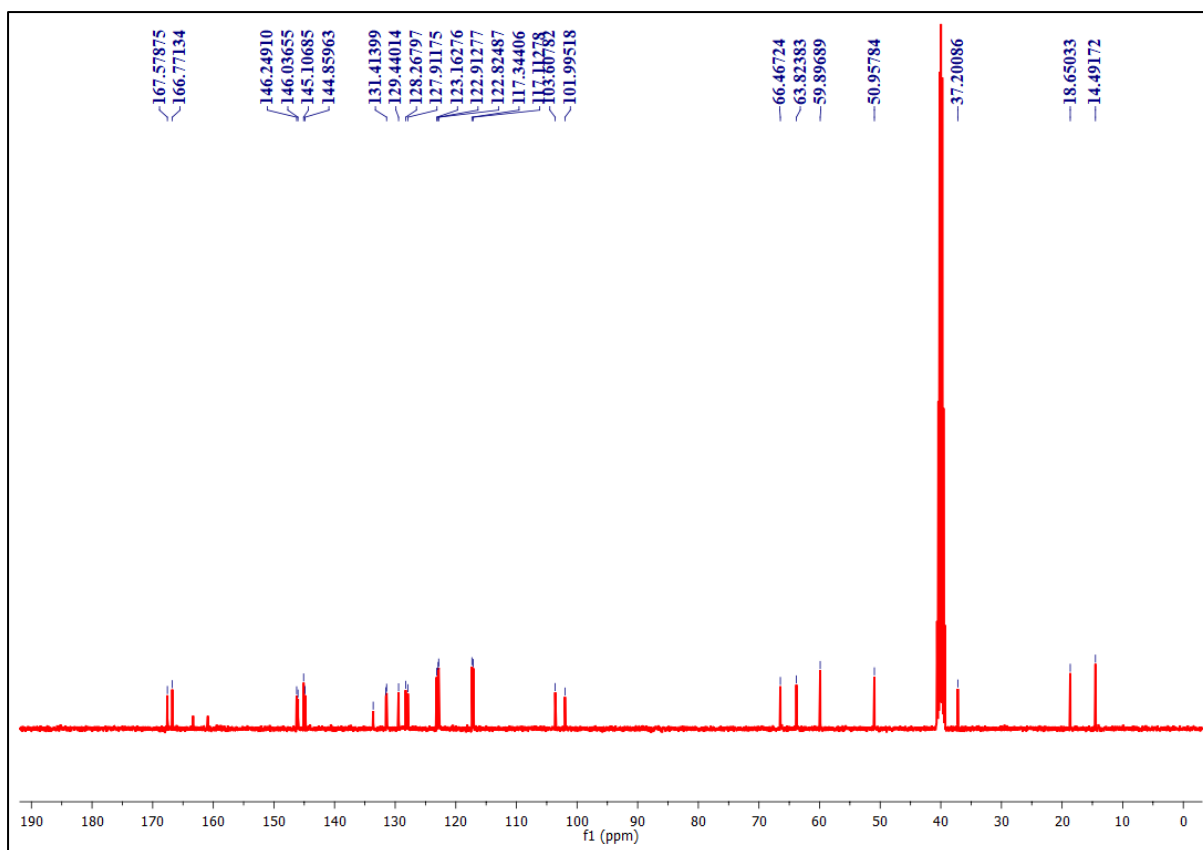


Figure S16. ^{13}C NMR spectrum of compound **P7** (100 MHz, $\text{DMSO-}d_6$).

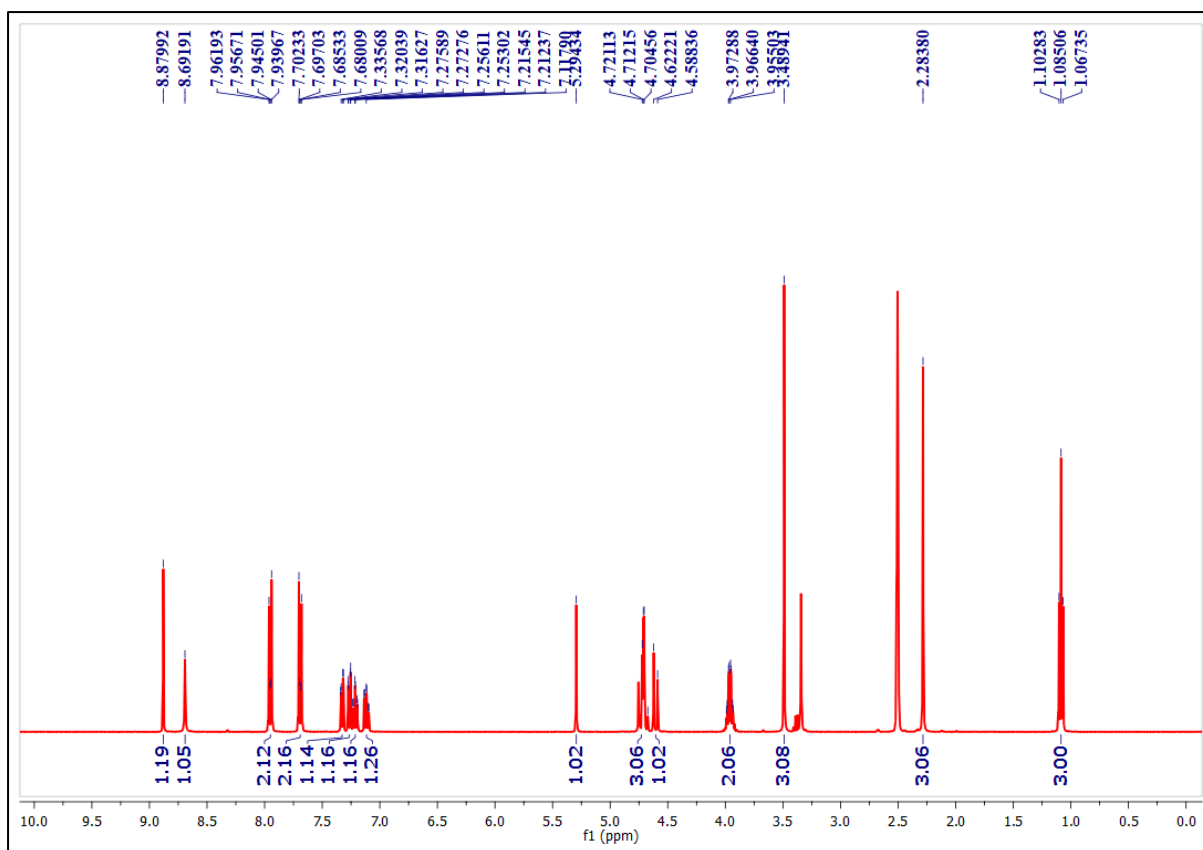


Figure S17. ¹H NMR spectrum of compound **P8** (400 MHz, DMSO-*d*₆).

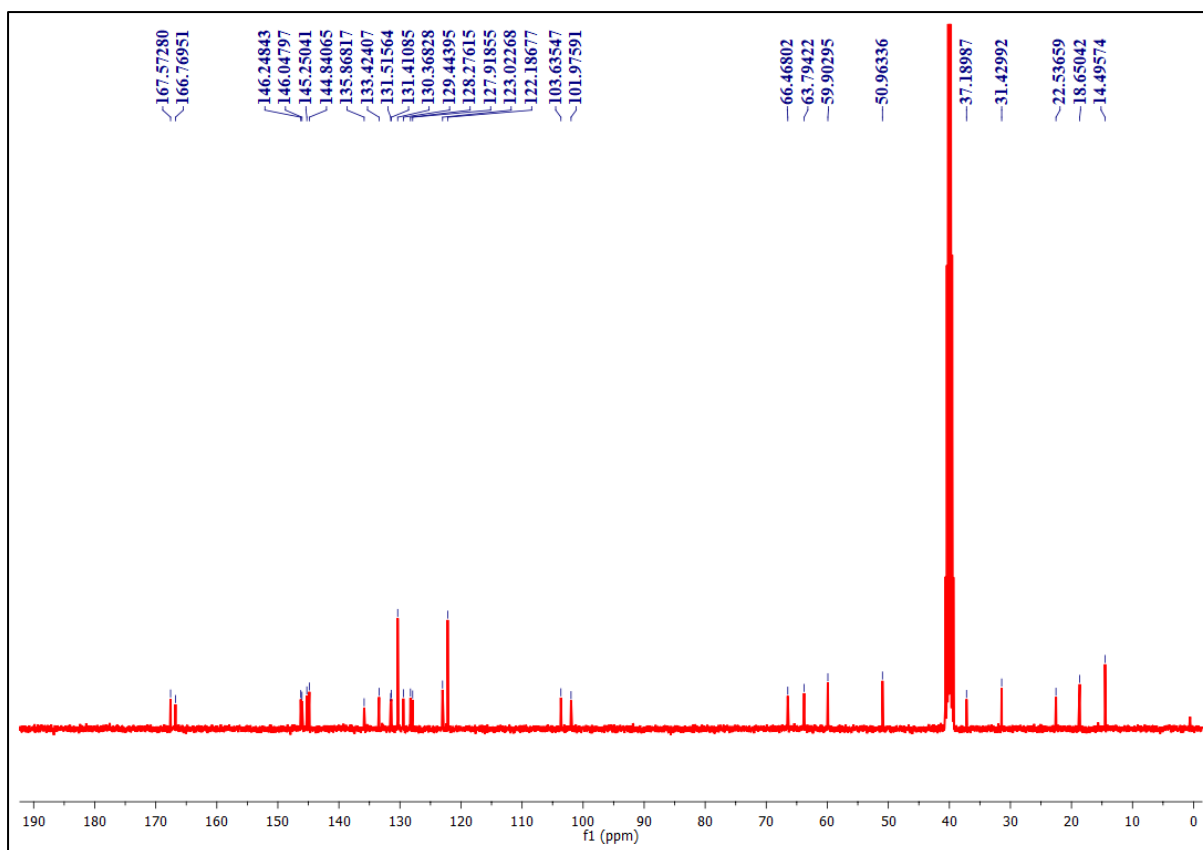


Figure S18. ^{13}C NMR spectrum of compound **P8** (100 MHz, $\text{DMSO-}d_6$).

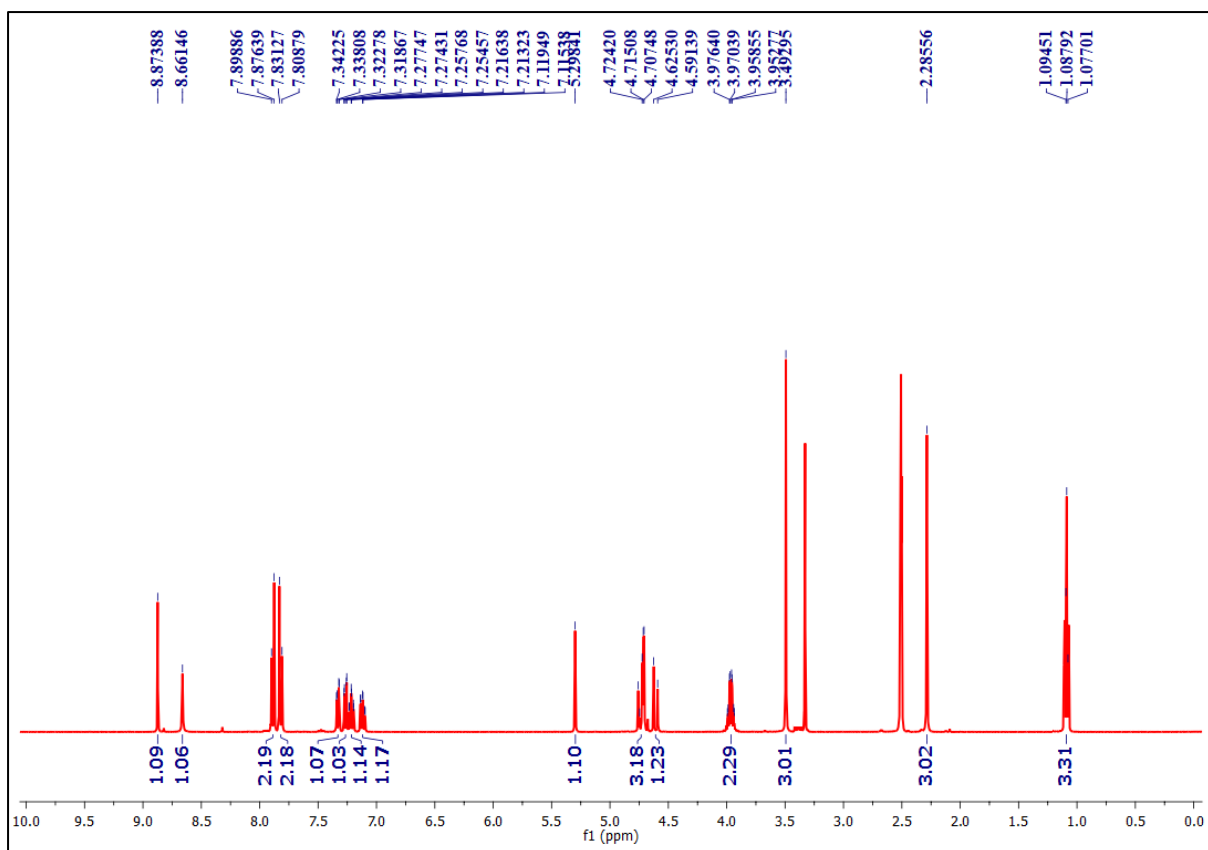


Figure S19. ^1H NMR spectrum of compound **P9** (400 MHz, $\text{DMSO-}d_6$).

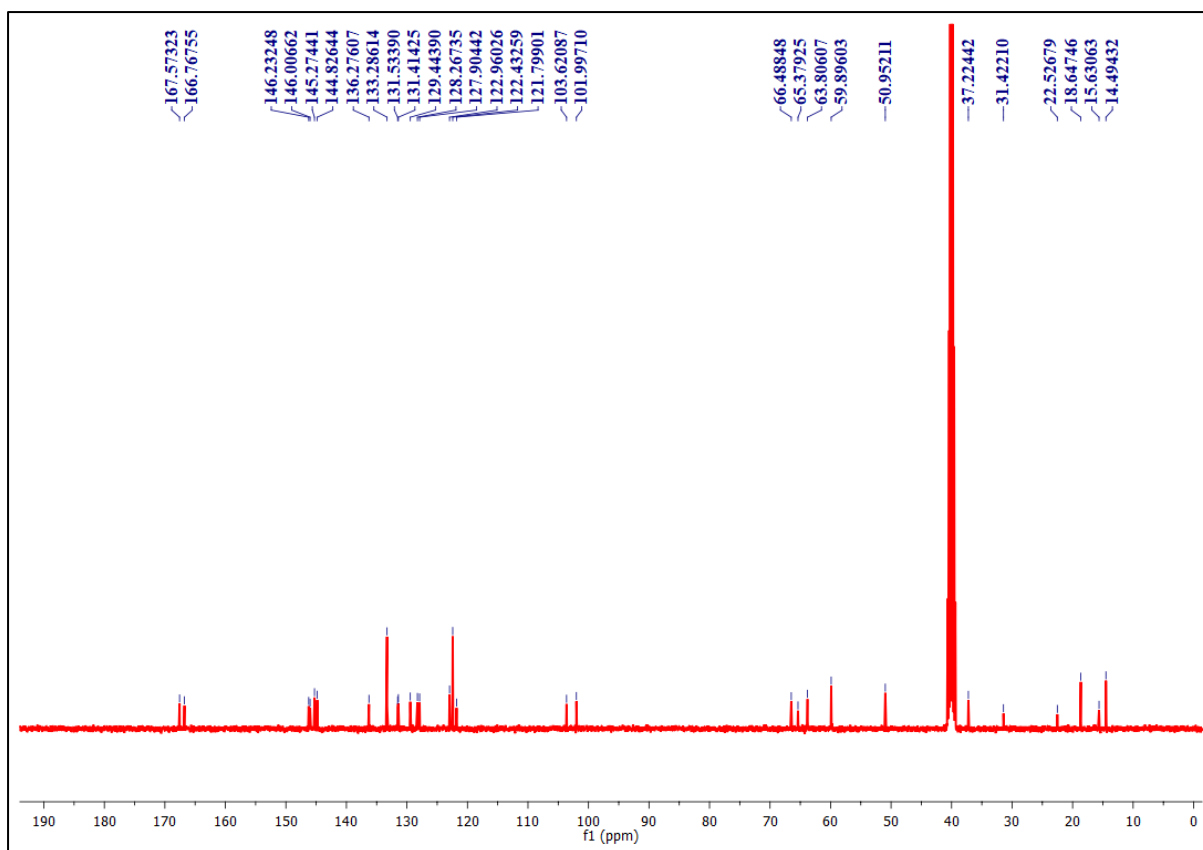


Figure S20. ^{13}C NMR spectrum of compound **P9** (100 MHz, $\text{DMSO-}d_6$).

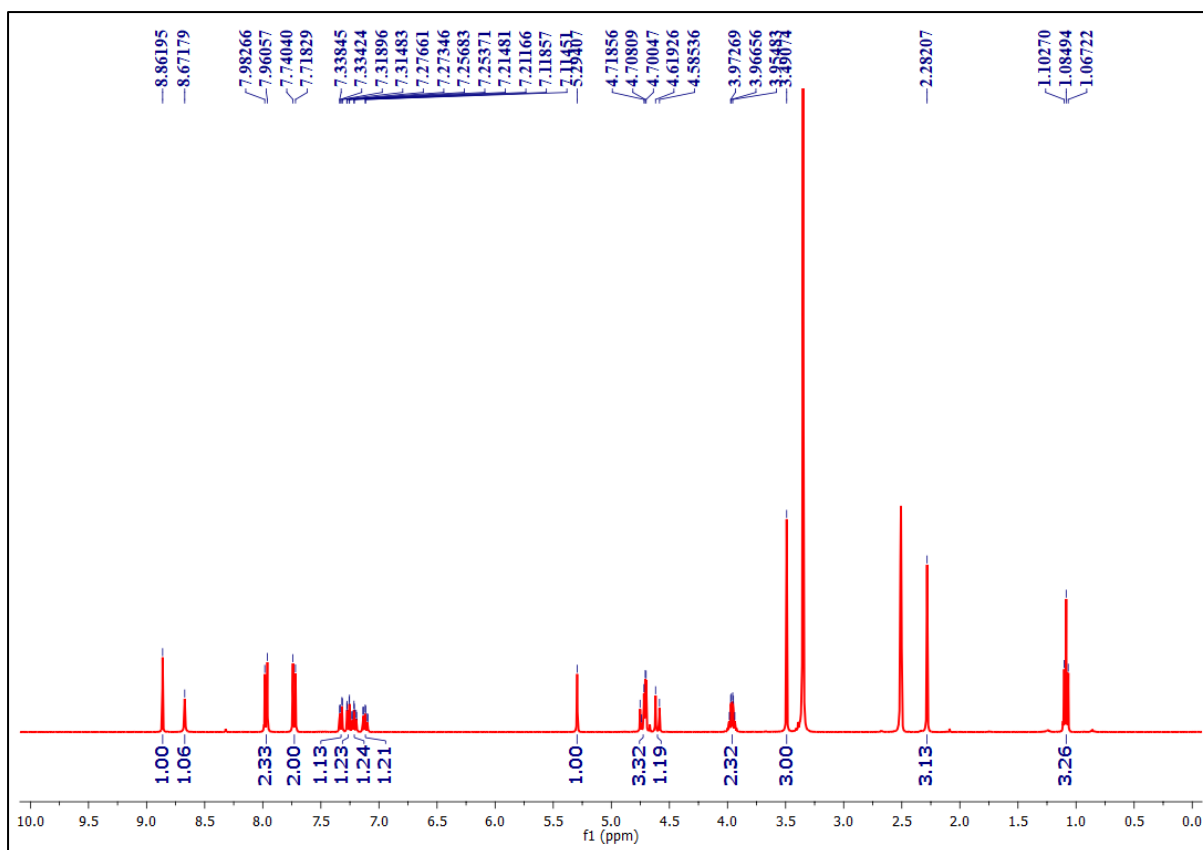


Figure S21. ^1H NMR spectrum of compound P10 (400 MHz, $\text{DMSO-}d_6$).

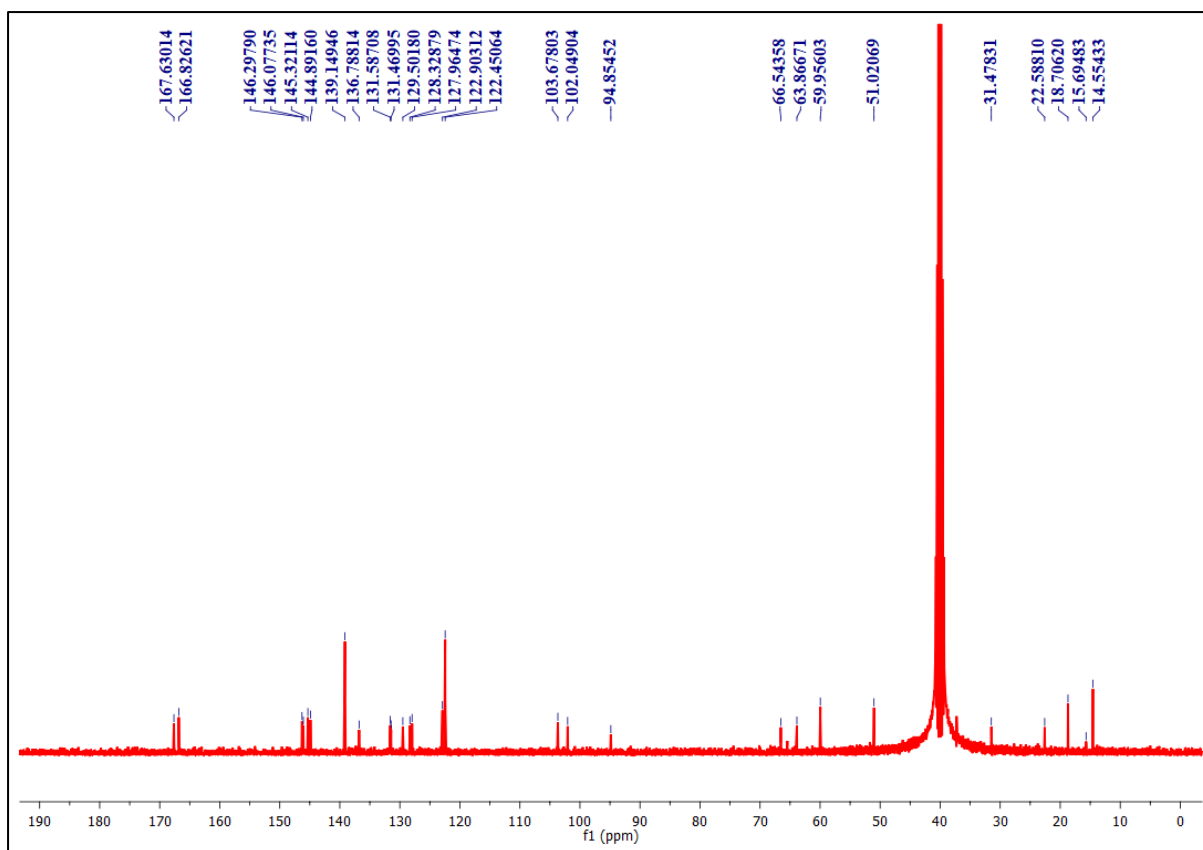


Figure S22. ^{13}C NMR spectrum of compound **P10** (100 MHz, $\text{DMSO-}d_6$).

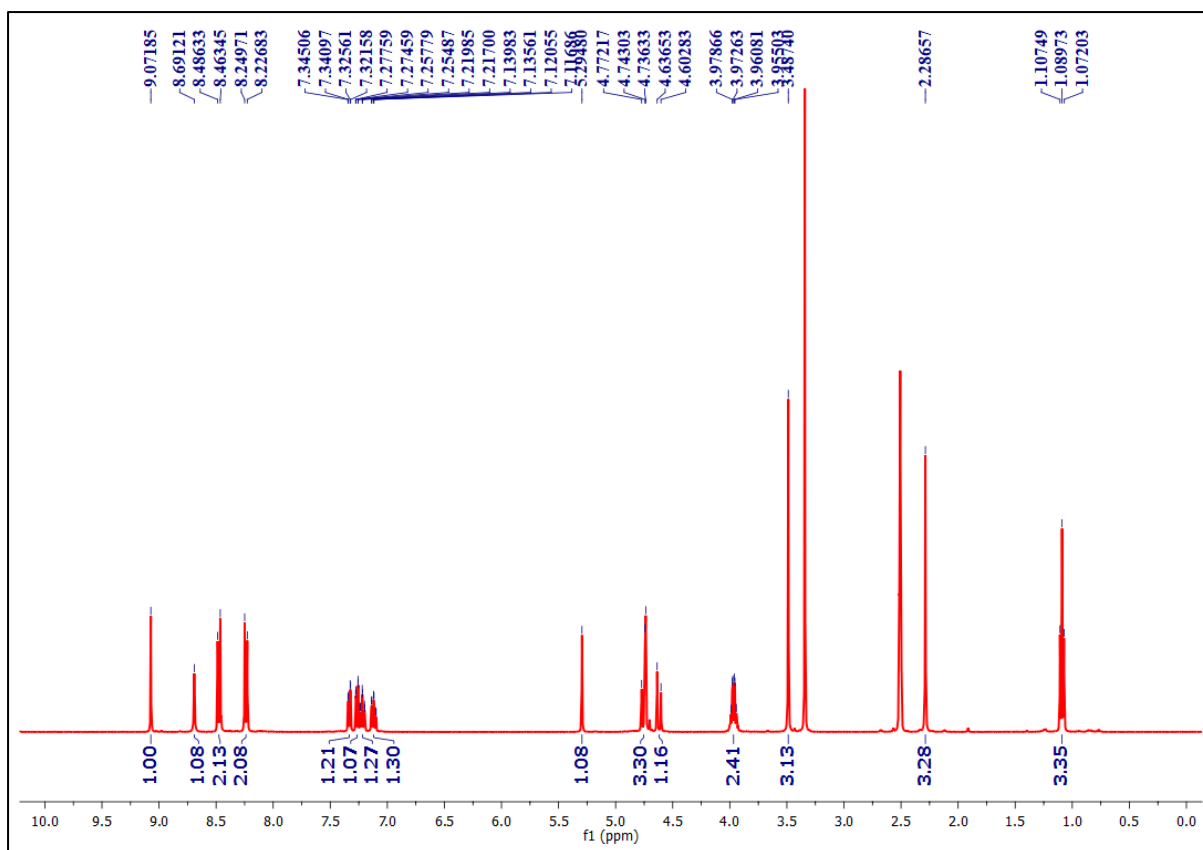


Figure S23. ¹H NMR spectrum of compound P11 (400 MHz, DMSO-*d*₆).

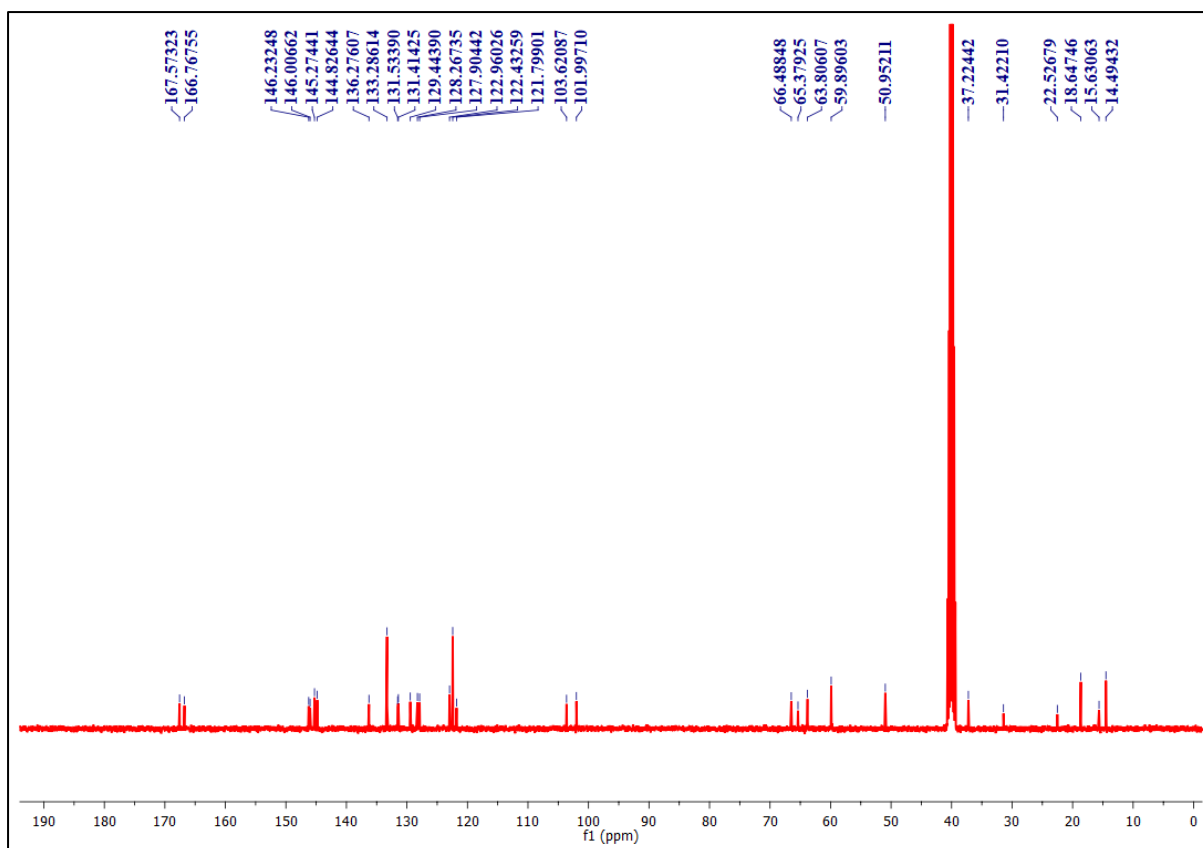


Figure S24. ^{13}C NMR spectrum of compound **P11** (100 MHz, $\text{DMSO-}d_6$).

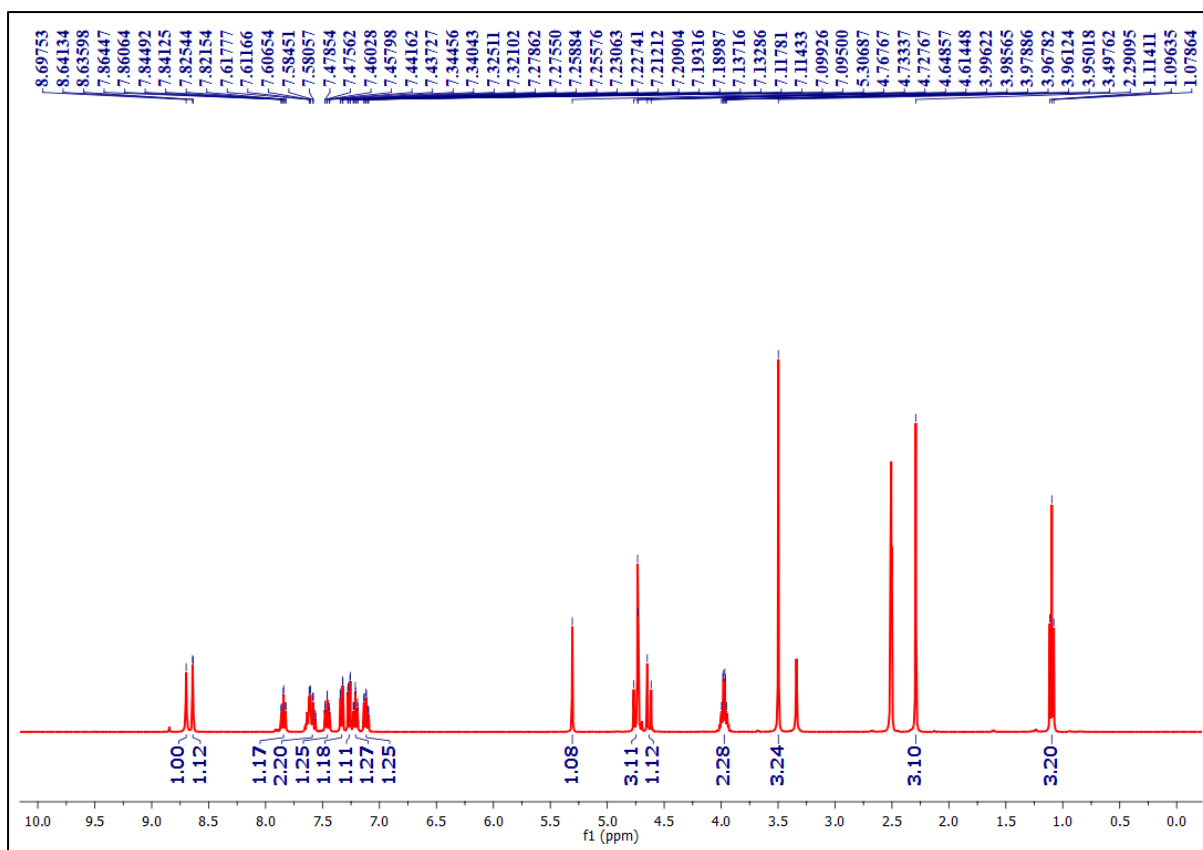


Figure S25. ^1H NMR spectrum of compound P12 (400 MHz, $\text{DMSO-}d_6$).

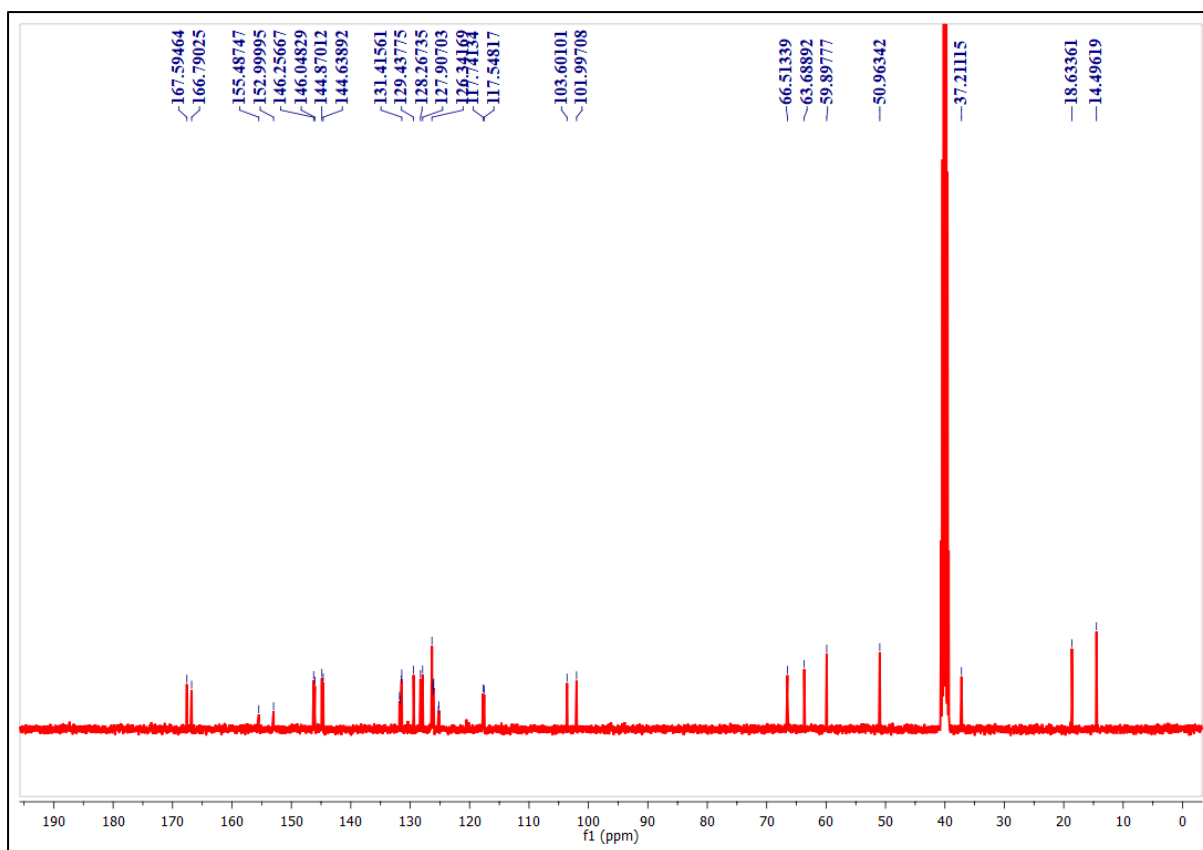


Figure S26. ¹³C NMR spectrum of compound P12 (100 MHz, DMSO-*d*₆).

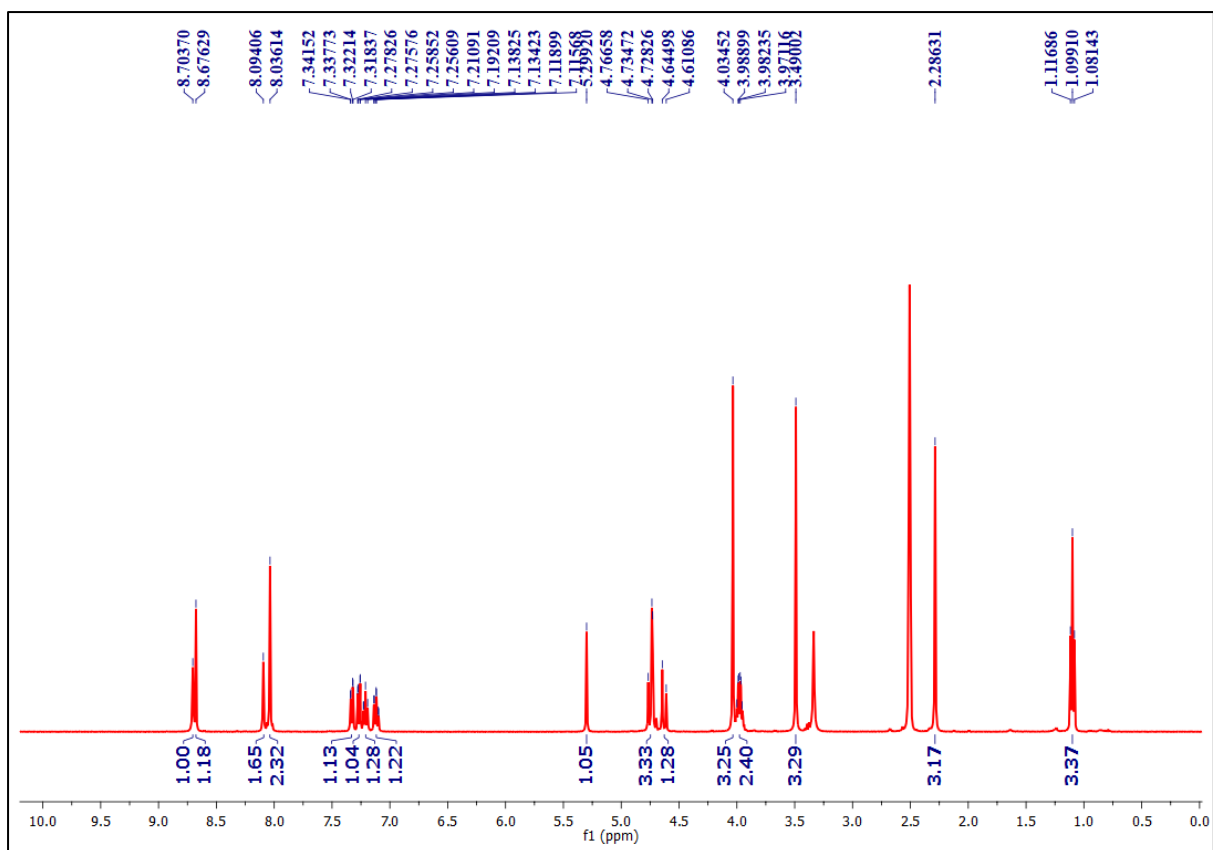


Figure S27. ^1H NMR spectrum of compound **P13** (400 MHz, $\text{DMSO-}d_6$).

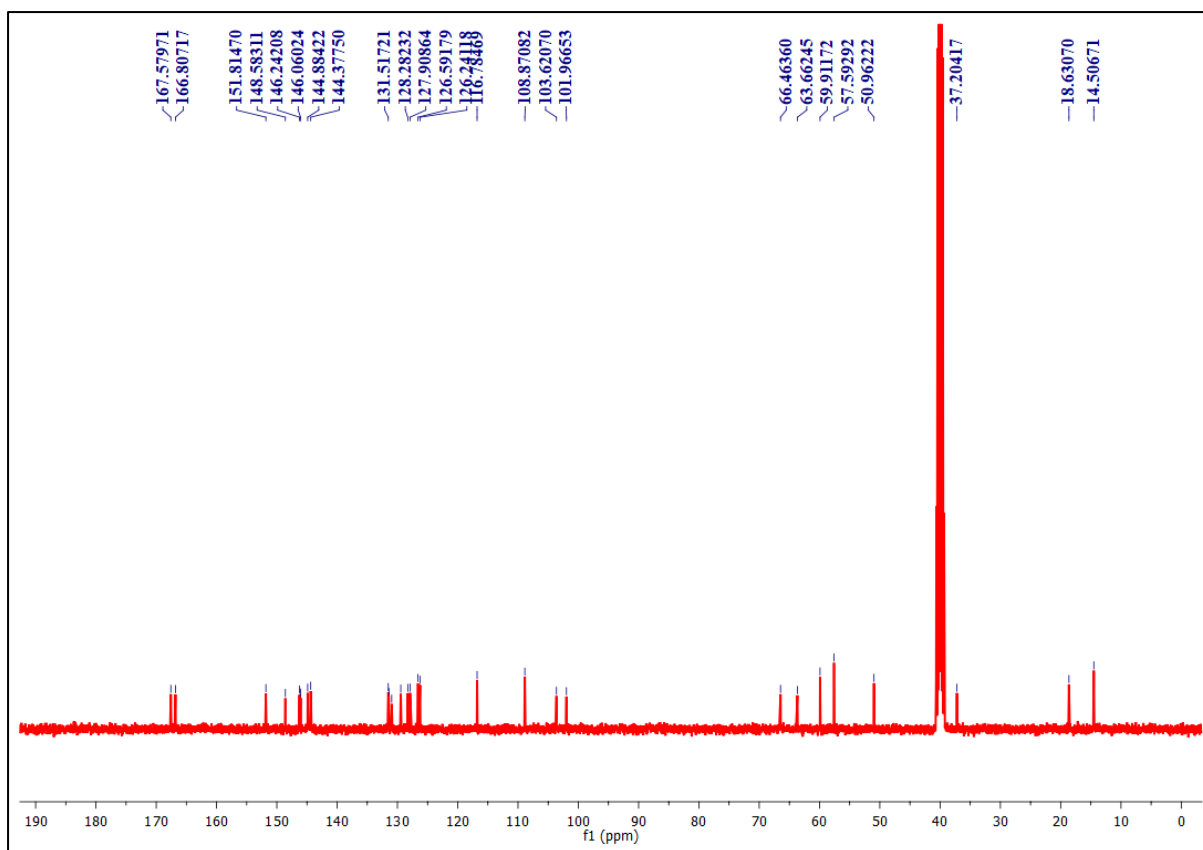


Figure S28. ^{13}C NMR spectrum of compound **P13** (100 MHz, $\text{DMSO-}d_6$).

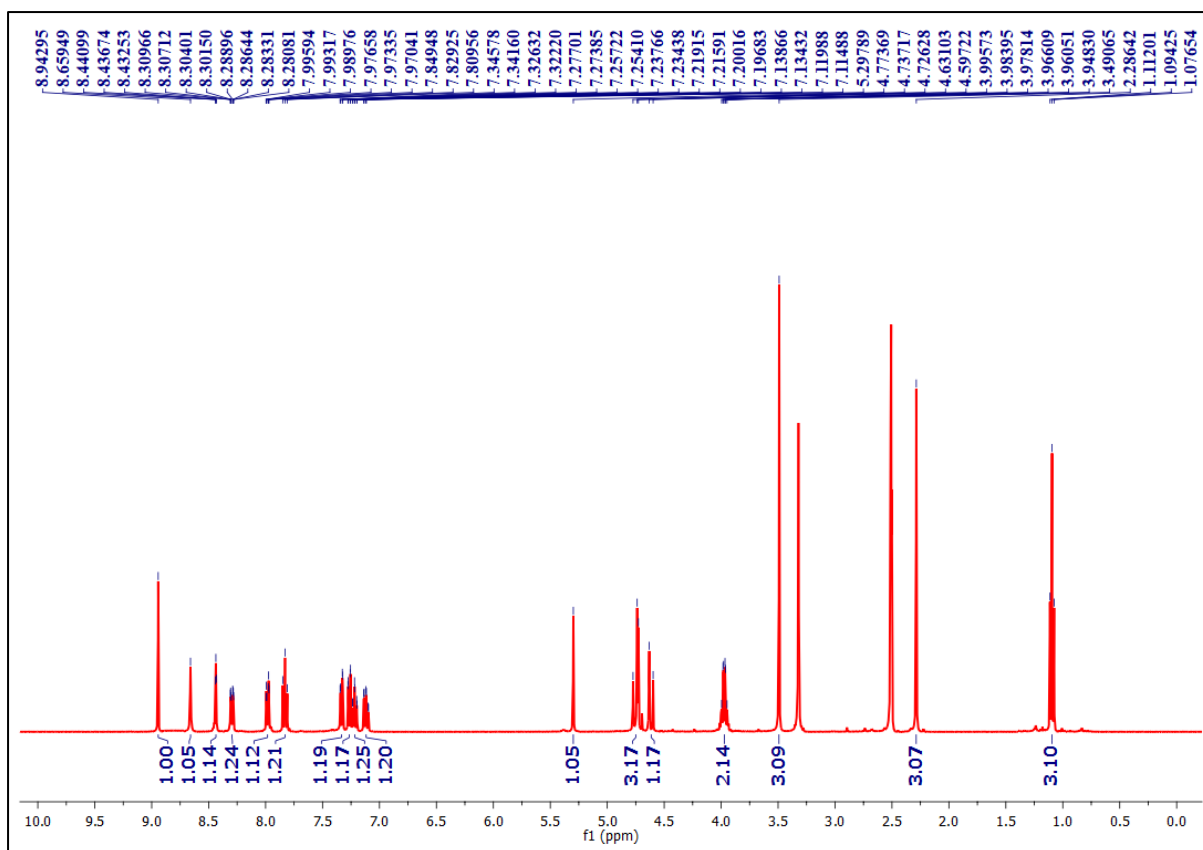


Figure S29. ^1H NMR spectrum of compound P14 (400 MHz, $\text{DMSO-}d_6$).

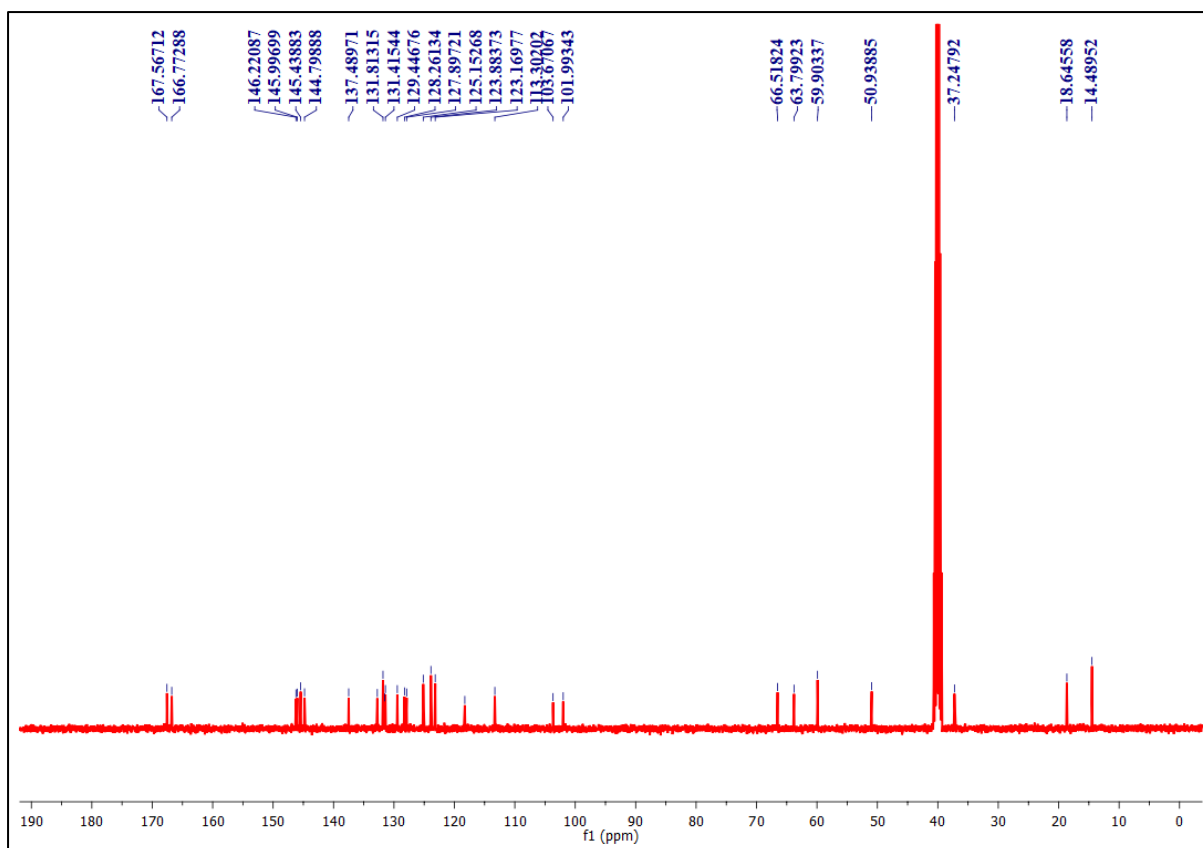


Figure S30. ^{13}C NMR spectrum of compound **P14** (100 MHz, $\text{DMSO-}d_6$).

3. Single crystal X-ray Structures:

Fine crystals of ligand **P7** were grown by slow evaporation of saturated mother solvent methanol & chloroform which was layered by hexane and diffused by ether at room temperature for SC-XRD studies. Good quality rectangular shaped yellowish crystals were taken and exposed to X-rays on a Bruker diffractometer employing a graphite monochromatized $\text{Mo/K}\alpha$ radiation ($\lambda = 0.71073 \text{ \AA}$) at temperature 107 K. The crystal data was reduced using CrysAlis pro software available with the diffractometer. Further, least square refinement after introduction of anisotropic displacement parameters yielded the R values mentioned in the **Table S1**. The structure was solved by direct methods using SHELXL-2016/4 and refined by the full-matrix least-squares method on Olex2.refine 1.5¹. All calculations were carried out using the OLEX2 package of the crystallographic programs². For the molecular graphics, the program Mercury (2022.3.0) was used³. The selected cell parameters, *etc.* are given in **Table S2**.

Table S1. Some important bond angles and bond lengths for **P7**.

Atoms	Bond Angle(°)	Atoms	Bond Length(Å)
∠ C00F–C00C–C11	124.9(1)	Cl–C00F	1.749
∠ C20–C00C–C11	118.4(1)	C00F–C00C	1.397
∠ C10–C11–C12	110.1(1)	C00C–C11	1.537
∠ O1–C8–C9	111.5(1)	C9–C8	1.524
∠ C7–O1–C8	113.2(1)	C8–O1	1.426
∠ O1–C7–C6	107.6(1)	O1–C7	1.436
∠ N2–C6–C5	108.5(1)	C7–C6	1.492
∠ N2–C6–C7	119.9(1)	N4–C00G	1.425
∠ C00G–N4–C5	129.5(1)	C00P–F	1.360
∠ N3–N4–C00G	119.9(1)	C9–C10	1.355

Table S2. Crystal data and structure refinement for compound **P7**

Identification code	S1
Empirical formula	C ₂₇ H ₂₆ Cl FN ₄ O ₅
Temperature/K	107(2)
Crystal system	monoclinic
Space group	P 21/c
a/Å	9.5711(4)
b/Å	37.8741(14)
c/Å	7.8420(3)
α/°	90
β/°	101.890(4)
γ/°	90
Volume/Å³	2781.71(19)
Z	31
ρ_{calc}/cm³	1.390
μ/mm⁻¹	0.192
F(000)	1224.0

Radiation	Mo/K α ($\lambda = 0.71073$)
2θ range for data collection/$^\circ$	3.059 to 31.063
Index ranges	$-12 \leq h \leq 13$, $-45 \leq k \leq 50$, $-8 \leq l \leq 10$
No of Reflections measured	7106
Independent reflections	5657
Goodness-of-fit on F2	1.097
R [F$^2 > 2\sigma$ (F2)], wR(all data)	0.0468, 0.1304

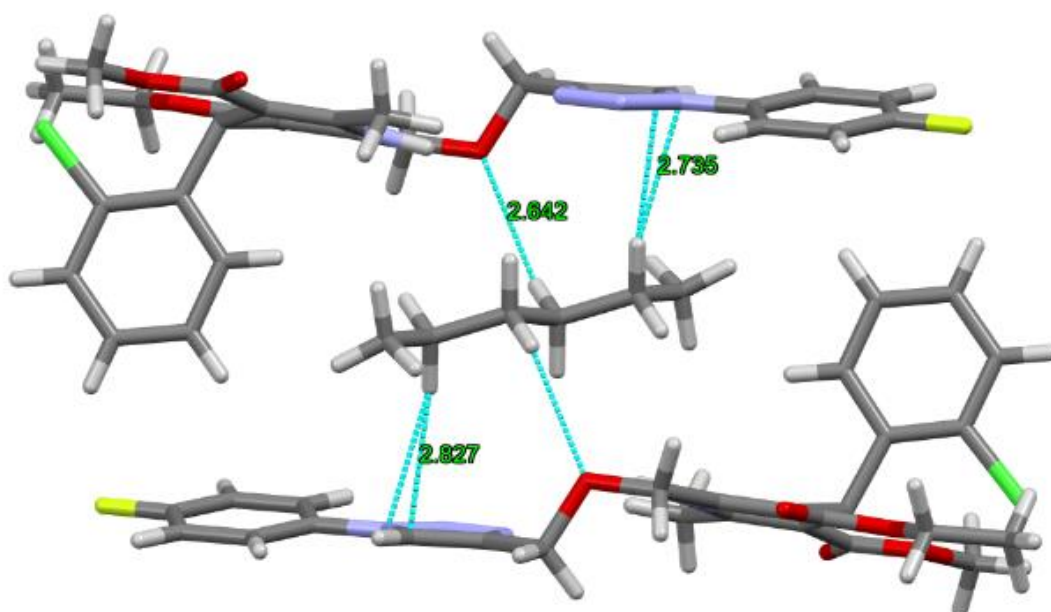


Figure S31. Host-guest encapsulation of solvent molecule via -CH-Pi interactions between the adjacent molecules of **P7**.

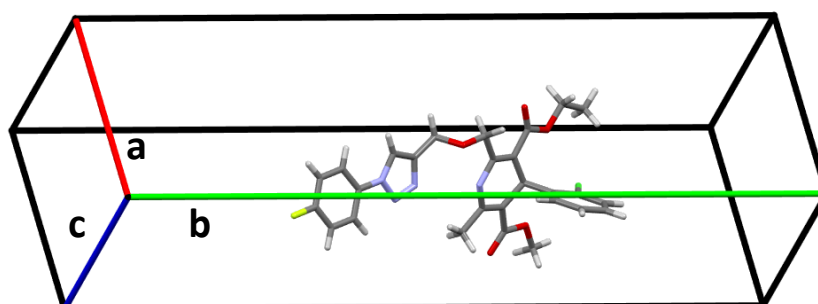


Figure S32. 3D packing arrangement of cell axis passing through the **P7** molecule.

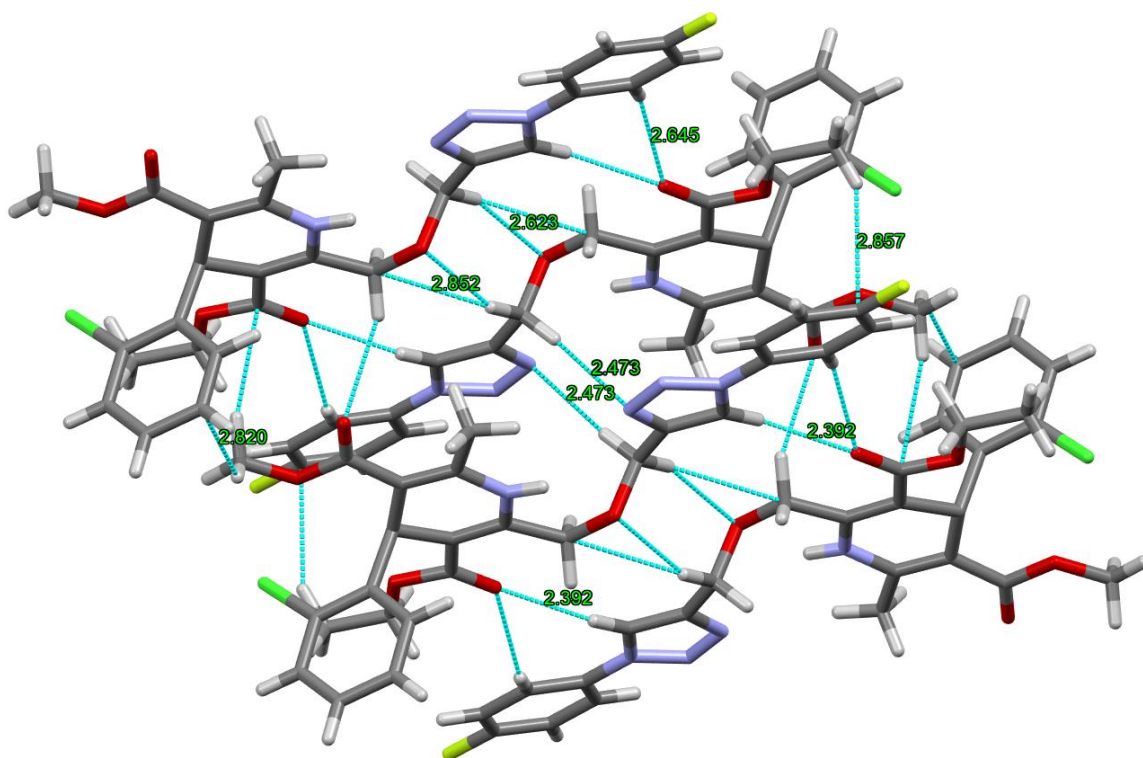


Figure S33. A network of **P7** via intra- and intermolecular H-bonding between the adjacent molecules.

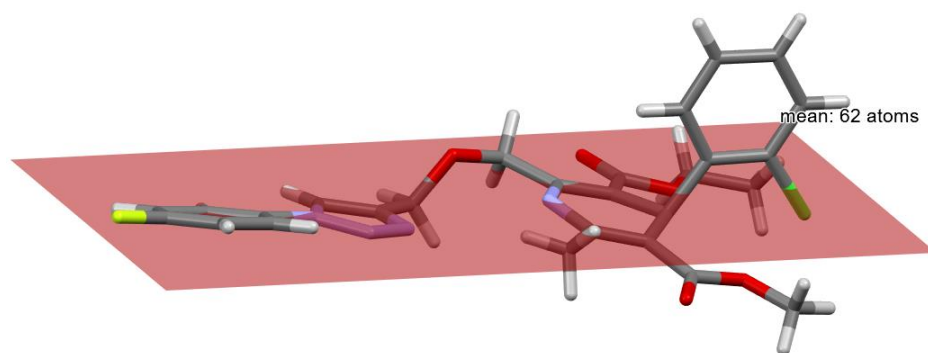


Figure S34. Gliding plane passing through the molecule for the confirmation of symmetrical and streamlined shape of the molecule **P7**.

4. Molecular Docking Assessment:

Table S3. Binding affinity of **P1-P14** with 5KMD along with their amino acid residue interactions.

Compound	Binding Affinity (kcal/mol)	Interacting amino acid residues
P1	-8.5	TYR1195, GLY1164, GLU1165, MET1188, PHE1167, ILE1199, THR1162, VAL1196, PRO1200, PHE1171, ARG1185, GLU1158, TYR1168
P2	-8.4	ILE1199, GLU1165, MET1188, ARG1185, TYR1168, TYR1195, VAL1196, PRO1200, PHE1171, PHE1167, GLU1158, GLU1189, THR1162, GLY1164
P3	-8.5	ILE1199, PHE1167, TYR1195, GLY1164, TYR1168, ARG1185, MET1188, GLU1165, PRO1200, PHE1171, VAL1196, THR1162, GLU1189, GLU1158
P4	-8.6	TYR1195, GLY1164, GLU1158, ARG1185, MET1188, GLU1165, PHE1167, ILE1199, VAL1196, PRO1200, PHE1171, THR1162, TYR1168
P5	-8.3	TYR1195, GLY1164, GLU1165, MET1188, PHE1167, ILE1199, VAL1196, PRO1200, PHE1171, ARG1185, GLU1158, TYR1168
P6	-7.6	TYR1195, PHE1167, ILE1199, GLY1164, PHE1171, PRO1200, VAL1196, TYR1168, MET1188, GLU1165
P7	-8.8	ILE1199, TYR1195, PHE1167, GLY1164, PHE1171, TYR1168, MET1188, GLU1165, VAL1196, PRO1200
P8	-7.9	ILE1199, PHE1167, TYR1195, GLY1164, TYR1168, MET1188, PHE1171, PRO1200, VAL1196, GLU1165
P9	-8.0	TYR1195, GLY1164, MET1188, PHE1167, ILE1199, VAL1196, PHE1203, PRO1200, PHE1171, TYR1168, GLU1165, GLU1158
P10	-7.8	MET1188, TYR1195, GLY1164, PHE1167, ILE1199, GLU1158, GLU1165, VAL1196, PRO1200, PHE1171, TYR1168

P11	-8.2	MET1188, GLY1164, TYR1195, PHE1167, ILE1199, ARG1185, GLU1158, GLU1165, TYR1168, LEU1163, PHE1171, PRO1200, PHE1203, VAL1196
P12	-7.8	ILE1199, PHE1167, TYR1195, GLY1164, PHE1171, THR1162, GLU1165, TYR1168, MET1188, VAL1196, PRO1200
P13	-7.6	MET1188, ARG1185, PHE1167, ILE1199, TYR1195, GLY1164, TYR1168, THR1162, PRO1192, GLU1165, GLU1158
P14	-8.1	ILE1199, GLY1164, PHE1167, TYR1195, ARG1185, MET1188, GLU1165, PHE1171, PHE1203, PRO1200, VAL1196, TYR1168, GLU1158
Amlodipine	-5.6	ILE1199, TYR1195, THR1138, VAL1196, PRO1200, PHE1203, PHE1141, PHE1167, PHE1171, TYR1168, GLY1164

Table S4. Binding affinity of **P1-P14** with 6M7H along with their amino acid residue interactions.

Compound	Binding Affinity (kcal/mol)	Interacting amino acid residues
P1	-8.1	LEU112, PHE19, LEU39, VAL91, ALA88, ASP80, MSE36, GLN41, GLU87, MSE72, PHE68, MSE145, MSE144, LEU105, MSE109, MSE124, PHE92, LEU18, VAL35, MSE71, ALA15
P2	-7.7	ASP80, LEU39, ALA88, PHE19, MSE144, MSE145, LYS75, GLU84, MSE36, PHE92, MSE109, MSE124, LEU18, PHE68, ALA15, MSE72, MSE71, VAL35, GLU87, GLN41, VAL91
P3	-7.2	ALA15, ALA88, LEU39, VAL91, MSE145, ASP80, GLU14, GLU11, LEU18, LEU112, GLN41, GLU87, VAL108, LYS75, MSE72, PHE68, MSE36, PHE19

P4	-8.0	ALA88, GLU84, PHE19, MSE144, MSE124, ALA128, VAL136, ILE100, PHE92, LEU112, GLU87, VAL91, LEU39, ILE125, MSE109, LEU18, PHE141, MSE36, MSE145, ILE85, ASP80, GLN41
P5	-8.3	LEU112, MSE124, MSE144, VAL136, PHE92, ALA128, LEU105, ALA88, GLU84, GLN41, LEU18, PHE19, MSE36, LEU39, VAL91, MSE145, GLU87, ASP80, PHE141, ILE100, ILE125, GLU127, MSE109
P6	-8.1	ALA88, MSE109, MSE145, ALA128, PHE92, ILE100, LEU105, MSE144, VAL136, ILE85, ASP80, GLU84, MSE36, GLN41, GLU87, LEU39, VAL91, ILE125, MSE124, PHE141, PHE19
P7	-8.3	ALA88, MSE109, MSE145, PHE92, ALA128, MSE144, LEU105, ASP80, PHE19, ILE85, MSE36, GLU84, GLU87, GLN41, VAL91, LEU39, MSE124, ILE125, VAL136, ILE100, PHE141
P8	-7.7	ALA88, MSE145, MSE109, MSE124, LEU105, PHE92, MSE144, VAL136, ILE125, ALA128, ILE85, ASP80, MSE36, PHE19, GLU84, GLN41, GLU87, VAL91, LEU39, PHE141, ILE100
P9	-7.4	ALA88, PHE92, MSE109, MSE124, ILE125, VAL136, ALA128, MSE144, LEU105, ASP80, MSE145, PHE19, GLU84, MSE36, GLU87, GLN41, VAL91, LEU39, PHE141
P10	-7.2	ALA88, ALA15, LEU18, GLU14, GLU11, PHE92, LEU39, VAL91, GLU87, GLN41, GLU84, MSE36, ILE85, ASP80, MSE145, PHE19, MSE109
P11	-7.7	ALA88, MSE109, MSE145, LEU105, ILE125, MSE144, PHE19, MSE36, ASP80, ILE85, GLU84, GLU87, GLN41, VAL91, LEU39, PHE92, ILE100, MSE124, VAL136, ALA128, PHE141
P12	-8.1	ALA88, MSE109, MSE145, MSE144, ALA128, ILE100, VAL136, PHE92, LEU105, ASP80, PHE19, MSE36,

		ILE85, GLU84, GLU87, GLN41, VAL91, LEU39, PHE141, ILE125, MSE124
P13	-7.4	ALA88, MSE109, MSE145, LEU105, MSE144, ILE125, ASP80, MSE36, ILE85, GLU84, GLN41, GLU87, VAL91, LEU39, PHE19, PHE92, PHE141, ILE100, VAL136, ALA128, MSE124
P14	-7.8	MSE144, MSE109, PHE92, ALA88, LEU105, MSE124, ALA128, ASP80, MSE145, ILE85, MSE36, PHE19, GLU84, GLU87, GLN41, VAL91, LEU39, ILE125, VAL136, ILE100, PHE141
Amlodipine	-5.1	ALA88, ILE85, GLU84, MSE36, GLN41, GLU87, VAL91, PHE92, LEU39, MSE145, PHE19, VAL35, LEU112, ASP80

5. In-silico ADMET Assessment:

In-silico ADMET (Absorption, Distribution, Metabolism, Excretion, and Toxicity) analysis is critical in the drug discovery and development as it predicts how a potential therapeutic compound will react in the body, particularly in the context of pharmacokinetics^{4,5}. ADMET assessments are conducted in conjunction with molecular docking investigations to assess the safety and efficacy of a pharmacological compound. In the journey of drug development, it is essential to examine the ADMET characteristics along with its adherence to the Lipinski rules⁶. Tables **S5** and **S6** present the critical pharmacological attributes of our newly synthesized candidates.

According to the Lipinski rules, an orally bioactive medication should ideally not exceed one violation. **Table S5** demonstrates that the synthesized compounds **P6-P10**, **P12**, and **P14** fully complied with the Lipinski criteria and no Lipinski violations were identified except one violation: MW>500. Further, compounds with their TPSA (Topological Polar Surface Area) values less than 140 Å² are anticipated to have a high oral bioavailability⁷. TPSA values of **P5-P10**, **P12**, and **P14** were determined to be <140 Å², suggesting their high oral bioavailability and hence can act as active therapeutic compounds. The TPSA values of the remaining scaffolds had a low oral bioavailability as depicted TPSA values exceeded the ideal value.

Furthermore, the in-silico results show moderate risk of hERG (human Ether-a-go-go-Related Gene) inhibition for all the hybrids except **P11**. Additionally, all the synthesized hybrids exhibited negative carcino test (mouse), that was found positive for the standard amlodipine. Whereas, all hybrids except **P9**, and **P10** displayed negative carcino test (rat), that was negative for amlodipine also. Thus, based on the negative carcino tests and moderate risk of hERG inhibition observed in the above assessments, it is indeed possible that these compounds might not lead to adverse cardiac implications.

Table S5. Drug-like properties of the synthesized hybrids **P1-P14**.

Compound	Molecular Formula	Molecular Weight	HBA*	HBD**	n. Rot.#	iLogP	Lipinski
P1	C ₃₁ H ₃₀ ClN ₅ O ₇	620.05	9	1	13	4.15	No; 2 violations: MW>500, NorO>10
P2	C ₃₁ H ₂₉ BrClN ₅ O ₇	698.95	9	1	13	4.40	No; 2 violations: MW>500, NorO>10
P3	C ₃₁ H ₂₉ Cl ₂ N ₅ O ₇	654.50	9	1	13	4.37	No; 2 violations: MW>500, NorO>10
P4	C ₃₁ H ₂₉ ClFN ₅ O ₇	638.04	10	1	13	3.85	No; 2 violations: MW>500, NorO>10
P5	C ₃₂ H ₃₂ ClN ₅ O ₆	618.08	8	1	14	4.42	No; 2 violations: MW>500, NorO>10
P6	C ₂₇ H ₂₇ ClN ₄ O ₅	522.98	7	1	11	4.42	Yes; 1 violation: MW>500
P7	C ₂₇ H ₂₆ ClFN ₄ O ₅	540.97	8	1	11	4.36	Yes; 1 violation: MW>500
P8	C ₂₇ H ₂₆ Cl ₂ N ₄ O ₅	557.43	7	1	11	4.50	Yes; 1 violation: MW>500
P9	C ₂₇ H ₂₆ BrClN ₄ O ₅	601.88	7	1	11	4.70	Yes; 1 violation: MW>500
P10	C ₂₇ H ₂₆ ClIN ₄ O ₅	648.88	7	1	11	4.68	Yes; 1 violation: MW>500
P11	C ₂₇ H ₂₆ ClN ₅ O ₇	567.98	9	1	12	4.18	No; 2 violations: MW>500, NorO>10
P12	C ₂₇ H ₂₆ ClFN ₄ O ₅	540.97	8	1	11	4.38	Yes; 1 violation: MW>500
P13	C ₂₈ H ₂₈ ClN ₅ O ₈	598.00	10	1	13	3.99	No; 2 violations: MW>500, NorO>10
P14	C ₂₈ H ₂₆ ClN ₅ O ₅	547.99	8	1	11	4.46	Yes; 1 violation: MW>500
Amlodipine	C ₂₀ H ₂₅ ClN ₂ O ₅	408.88	6	2	10	3.17	Yes; 0 violation

* HBA = Hydrogen Bonded Acceptors; ** HBD = Hydrogen Bonded Donors; # n. Rot. = Number of rotatable bonds

Table S6. ADMET properties of the synthesized hybrids **P1-P14**.

Compound	GI Absorption	BBB permeant	TPSA	Synthetic Assessability	PAINS Alerts	Carcino Test(Mouse)	Carcino Test(Rat)	hERG inhibition
P1	Low	No	141.95	5.15	0	negative	negative	Medium risk
P2	Low	No	141.95	5.19	0	negative	negative	Medium risk
P3	Low	No	141.95	5.15	0	negative	negative	Medium risk
P4	Low	No	141.95	5.17	0	negative	negative	Medium risk
P5	Low	No	126.57	5.21	0	negative	negative	Medium risk
P6	High	No	104.57	4.79	0	negative	negative	Medium risk
P7	High	No	104.57	4.77	0	negative	negative	Medium risk
P8	High	No	104.57	4.80	0	negative	negative	Medium risk
P9	High	No	104.57	4.79	0	negative	positive	Medium risk
P10	High	No	104.57	4.85	0	negative	positive	Medium risk
P11	Low	No	150.39	4.87	0	negative	negative	High risk
P12	High	No	104.57	4.76	0	negative	negative	Medium risk
P13	Low	No	159.62	5.04	0	negative	negative	Medium risk
P14	High	No	128.36	4.84	0	negative	negative	Medium risk
Amlodipine	High	No	99.88	4.39	0	positive	negative	Medium risk

6. BOILED Egg Plot Analysis:

It is imperative to investigate the two significant pharmacokinetic aspects of a compound throughout the multiple phases of drug discovery: its gastrointestinal absorption and its ability to penetrate the brain⁸. These assessments provide critical insights into how the compound is absorbed in the digestive tract and whether it can cross the blood-brain-barrier, which significantly impacts its suitability as a prospective therapeutic candidate. We assessed the gastrointestinal absorption (GI) and blood-brain-barrier (BBB) permeation attributes of the synthesized hybrids using the BOILED-Egg approach⁹. The resulting graph, as shown in **Fig. S35**, depicts the findings of this analysis. In this approach, the white region corresponds to the physicochemical field associated with the compounds that can be effectively absorbed by the GI tract. Conversely, the yellow region signifies the physicochemical field associated with the compounds having the potential to permeate the BBB (blood-brain-barrier), implying their capability to access the central nervous system (CNS). These findings are essential to understand the potential pharmacokinetic behaviour of the compounds and their capacity to reach target sites throughout the body. As evident from Table and Figure, compounds **P6-P10**, **P12** and **P14** exhibit high gastrointestinal absorption and no blood-brain-barrier penetration, which is noticeable in the white region of the egg. However, compounds **P1-P5**, **P11** and **P13** were found to have low GI absorption and were not able to penetrate the BBB.

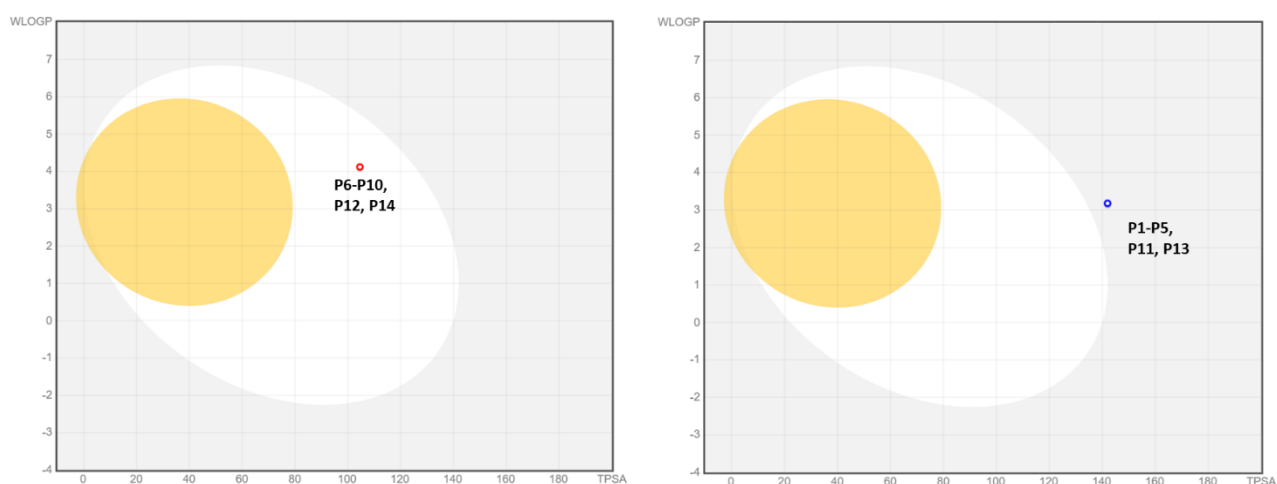


Fig. S35. BOILED Egg plot analysis demonstrating high GI absorption in case of compounds **P6-P10**, **P12** and **P14** as depicted in the white region of the egg and low GI absorption in case of **P1-P5**, **P11** and **P13**.

References

- 1 G. M. Sheldrick, *Acta Crystallogr. Sect. C Struct. Chem.*, 2015, **71**, 3–8.
- 2 O. V Dolomanov, *J. Appl. Cryst.*, 2009, **42**, 339–341.
- 3 C. F. Macrae, P. R. Edgington, P. McCabe, E. Pidcock, G. P. Shields, R. Taylor, M. Towler and J. V. D. Streek, *J. Appl. Crystallogr.*, 2006, **39**, 453–457.
- 4 S. Kar and J. Leszczynski, *Expert Opin. Drug Discov.*, 2020, **15**, 1473–1487.
- 5 G. Moroy, V. Y. Martiny, P. Vayer, B. O. Villoutreix and M. A. Miteva, *Drug Discov. Today*, 2012, **17**, 44–55.
- 6 C. A. Lipinski, *Drug Discov. today Technol.*, 2004, **1**, 337–341.
- 7 J. J. Lu, K. Crimin, J. T. Goodwin, P. Crivori, C. Orrenius, L. Xing, P. J. Tandler, T. J. Vidmar, B. M. Amore and A. G. E. Wilson, *J. Med. Chem.*, 2004, **47**, 6104–6107.
- 8 H. A. Alghamdi, S. A. Attique, W. Yan, A. Arooj, O. Albulym, D. Zhu, M. Bilal and M. Z. Nawaz, *Process Biochem.*, 2021, **110**, 216–222.
- 9 A. Daina and V. Zoete, *ChemMedChem*, 2016, **11**, 1117–1121.